ISSN 2961-7855

REE

Frontiers in Renewable Energy

Volume 1 Number 1 August 2022

Published by
Center for Energy Studies
Universitas Gadjah Mada

Editorial Message

On behalf of the Board, I am delighted to announce the launch of the first issue of the *Frontiers in Renewable Energy* (FREE). FREE is an international journal covering fundamental to advanced renewable energy technologies, policies, and economics. This journal has been nearly two years in the making, as a culmination of thoughts from our energy experts in Center for Energy Studies (CES), Universitas Gadjah Mada. It was felt that by hosting an international journal was an ideal vehicle to spread our academic contribution in renewable energy area. Then, in 2021 the board was established with Prof. Deendarlianto as Editorial-in-chief and Dr. Roni Irnawan as the managing editor along with Dr. M Mufti Azis, Dr. Nugroho Dewanto, and Dr. Hifni Mukhtar Ariyadi. The board decided that the journal should be published as an open-access online journal, such that the content can be accessed easily.

In this first issue we have six papers covering different topics in PEM electrolyzer, bio-crude oil, lipid extraction, and slug flow in horizontal pipes. These papers have been through reviewing processes by expert in those fields from around the globe. In the next issue we expect to have papers from different aspect like:

- Renewable energy sources implementation in archipelagic areas
- Renewable energy source and system, such as biofuel, biomass, geothermal energy, hydropower, solar energy, wind power, etc
- Application of renewable energy source and system
- Novel energy conversion for renewable energy source and system
- Artificial intelligent studies in renewable energy source and system
- Future direction of renewable energy source and system
- Sustainable and clean energy issues
- Policies and strategies for renewable energy source and system
- Integration of renewable energy sources
- Energy transition

The birth of FREE comes after a long process and we committed to took all the necessary steps to make it a high reputable journal. We are relying on the collaboration of all our Editors, reviewers and contributors to make it a contemporary, lively and relevant publication.

We hope you will enjoy reading our first issue, and that you find these articles useful to stimulate your research. We invite you to submit your best papers for publication.

Best regards,

Prof. Deendarlianto
Editor-in-chief
Center for Energy Studies, UGM

Table of Contents

FREE 1 (2022) 1-12

Frontiers in Renewable Energy (FREE)

Journal homepage: www. https://jurnal.ugm.ac.id/v3/FREE/

Mathematical Modeling of Hydrodynamic Cavitation as Low Energy Extraction Technique to Remove Lipid from Nannochloropsis sp.

Martomo Setyawan[1,2], Panut Mulyono[2], Sutijan[2], Razif Harun[3] and Arief Budiman[2,4,*]

[1] Faculty of Industrial Engineering, Ahmad Dahlan University, Jalan Prof DR Soepomo SH Yogyakarta, Indonesia
[2] Chemical Engineering Department, Gadjah Mada University, Jalan Grafika 2 Yogyakarta, Indonesia
[3]Department of Chemical and Environmental Engineering, Universiti Putra Malaysia, 43400 Serdang Selangor, Malaysia
[4] Center for Energy Studies, Gadjah Mada University, Sekip K IA, Yogyakarta, Indonesia

ARTICLE INFO

Article history:
Received 21 January 2022
Revised 4 February 2022
Accepted 8 April 2022
Available online 10 August 2022

Key words:

Hydrodynamic cavitation, Lipid extraction, Microalgae, Energy of extraction, Mathematical modeling

ABSTRACT

Lipid extraction through hydrodynamic cavitation (HCLE) is one of the promising processes with low energy requirements. Therefore, this study focuses on reducing energy requirements using a discrete flow system as well as evaluating two models to be used in calculating volumetric mass transfer coefficient. It was discovered that the variations in the number of repetitions, cavitation number, microalgae concentration, and temperature affected the energy requirement value and the lowest energy requirement was recorded to be 10 kJ/gram lipid. Moreover, the first model was designed using total lipid mass transfer approximation (Model 1) while the second was through separated lipid mass transfer approximation (Model 2). It was found that the extraction curve consists of three sections and the values of total volumetric mass transfer coefficient ($k_T a_T$) for sections 1, 2, and 3 based on Model 1 were 1.166 x 10^{-2}, 3.113 x 10^{-3}, and 1.285 x 10^{-3} min^{-1} with a coefficient of determination (R^2) of 0.9797, respectively. Meanwhile, the values of volumetric mass transfer coefficient from disrupted microalgae ($k_f a_o$) for sections 1, 2, and 3 based on Model 2 were 1.131 x 10^{-2}, 2.925 x 10^{-3}, and 1.260 x 10^{-3} min^{-1} respectively, and from the intact microalgae ($k_s a_s$) was 0.051, 0.030 and 0.011 1/min with R^2 of 0.9766. This means the two models showed similar results and the lipid released from the disrupted microalgae was observed to be dominant compared to the intact microalgae. Therefore, the discrete flow system of HCLE is a promising technique to be developed and scaled up to extract lipids from microalgae.

I INTRODUCTION

The increasing human population and modern human lifestyle have increased energy demand and this is currently mostly fulfilled through the reliance on petroleum resources. This has created some global energy problems due to the contradiction between the demand and supply [1], [2] as indicated

Peer review under responsibility of Frontiers in Renewable Energy (FREE).
*Corresponding author.
E-mail address: abudiman@ugm.ac.id (Arief Budiman)
0001-00012/ 2022. Published by Frontiers in Renewable energy (FREE).

by the continuous increase in demand with a reduction in the stocks of petroleum resources considered to be non-renewable. Another important problem is the occurrence of global warming due to greenhouse gas emissions such as carbon dioxide. This led to the proposition of some solutions such as the application of new and renewable energy resources such as biomass and vegetable oil to fulfill energy demands in the future. This is expected to solve energy and environmental problems because of the need to grow carbon dioxide to produce these energy resources, thereby, forming a closed chain of carbon [3], [4].

Some potential problems have, however, been observed in relation to the use of biomass and vegetable oil as energy resources and these include threats against food and land security. This is the reason it is preferable to select either a non-edible vegetable oil or biomass waste to serve as energy resources [5]. Previous studies have investigated some fuels produced from non-edible and waste renewable resources such as bio-oil from palm empty fruit branch (EFB) [6], biodiesel from palm fatty acid distillate [7], biodiesel from cooking oil waste [8], gas from sugarcane bagasse [9], bio-oil from woods, vegetables, and fruits waste [10], bio-oil from microalgae waste [11] and biodiesel from non-edible seeds such as jatropha and papaya seed [12]. In recent times, the production of the third generation of biodiesel from microalgae lipid has also been investigated [5].

Microalgae have been proved to be a potential feedstock to produce future energy due to their numerous attractive features such as higher productivity and oil content than other energy crops. Moreover, the lower consumption of freshwater and utilization of arable land to obtain microalgal biomass ignite research interest to exploit them for product development such as biofuel [13]. Most importantly, these microalgae use carbon dioxide for photosynthesis, thereby, leading to the reduction of global warming effects. They also have other added value in the form of biomass waste that can be used to produce bio-oil in addition to their oil content which can be used to produce energy [11].

Previous studies on biodiesel production from microalgae concluded that microalgal biodiesel is not profitable at an industrial scale [14], [15] due to the higher extraction energy required compared to the potential energy from biodiesel. This high-energy input accounts for more than 30% of the total cost of extracting lipids and this makes the current commercial microalgal biofuel production economically unfeasible. It has also been reported that the energy required to extract microalgal lipid mechanically is approximately 529 $kJ.g^{-1}$ dry microalgae [16] and the lowest is 3 $kJ.g^{-1}$ dry microalgae while the High Heating Value (HHV) of the biodiesel is only 42 $kJ.g^{-1}$ [17]. This means the lowest energy needed to achieve a 10% g/g yield is 30 $kJ.g^{-1}$. This comparison shows that extraction energy requirement plays is very important in providing enough gap to obtain both positive and large net energy to be consumed for further processing.

The most conventional extraction techniques of microalgal lipids involve longer processing steps, time, and sometimes high energy consumption and this hinders the full commercialization of lipids products [18]. Therefore, there is a need for an economical, fast, and robust approach to extracting lipids from microalgae. It is important to note that microalgae cell disruption is a major factor in maximizing extraction yields [19] and one of the extraction methods with much lower energy and the ability to produce a considerably high amount of lipid is hydrodynamic cavitation [20]. This technique provides a fast extraction rate [21] and low energy cell disruption using cavitation generated by dropping flow pressure through an increment in flow velocity [16] [22], thereby, making it easy to scale up this method [23]. It is also important to reiterate that hydrodynamic cavitation follows a solid-liquid mass transfer principle due to the cell disruption process and the initial concentration of microalgae is observed to be a crucial factor in improving the efficiency of the lipid recovery process. Moreover, higher microalgal concentration also affects the rate of solid-liquid mass transfer [24] and this led to the recommendation of distribution between 5% to 10% gram microalgae per gram of feed mixture [23]. This present study focuses on investigating the

correlation between the initial concentration and convective mass transfer parameters during the extraction of microalgal biomass via a discrete flow system of hydrodynamic cavitation. The energy required was measured and mathematical modeling was subsequently developed to understand the overall extraction process.

II MATERIALS AND METHODS

2.1 Microalgae

The microalgae used in this experiment is Nannochloropsis sp which was purchased from Balai Budidaya Air Payau in Situbondo East Java Indonesia and delivered in green powder which was stored in a desiccator and used as received for further analysis.

2.2 Solvents

The solvents used in this experiment include n-hexane (PT. Brataco Chemica, Indonesia, MW 86.18, 99.5%), and methanol (CV. Multi Kimia, Indonesia, MW 32.04, 99.5%) selected based on their non-ideal properties in terms of the boiling point when mixed. The mixture of 95 ml hexane and 41 ml methanol has a boiling point lower than their respective separate boiling points as indicated by 52, 64.96, and 68.73 ^{o}C for the mixture, methanol, and hexane respectively.

2.3 Equipment

The experiments were conducted using a batch discrete flow system of hydrodynamic cavitation using a unit that consists of a compressor, sample chamber, venturi, and product chamber as shown in Figure 1. The compressor was used to supply compressed air and drive the solvent-sample mixture to the sample chamber. The venturi was used to generate cavitation while the sample and product chamber was employed to store feedstock and collect products. At the end of the process, the centrifuge was used to separate the fluid from solid products and the distillator to separate the solvent from lipid by evaporating the solvent.

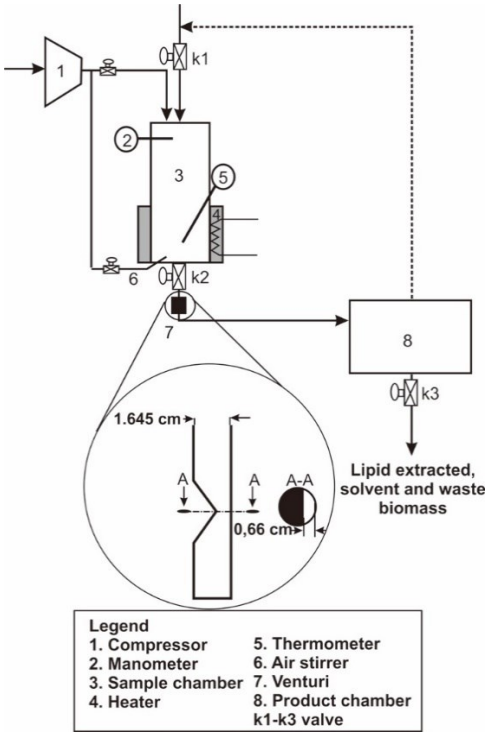

Figure 1. The Scheme of Hydrodynamic Cavitation Equipment.

2.4 Experimental Procedures

The HCLE discrete flow system experiments were conducted by varying the microalgae concentration, cavitation number, and temperature. The *Nannochloropsis sp*. biomass was varied at 5, 7.5, 10, and 12.5 grams, the cavitation number at different pressure boosters of 3.125, 4.167, 5, and 6.25 atm, the temperature at 30, 34, 38, 42, 46, and 50 °C. It is important to restate that a mixture of methanol and hexane was used as the extraction solvent. The biomass and solvents were loaded into the sample chamber, flowed through the venturi with a pressure booster, and the mixtures were re-flowed at 2, 3, 4, and 5 cycles to study the degree of cell disruption and lipid yields. The completion of the extraction process was followed by the separation of the extracts and solid phase using the centrifugation process. Moreover, the solids were washed with an equal amount of methanol and hexane to ensure all the lipids extracted from the microalgae were retrieved and weighed and those dissolved in the mixture solvent were recovered as a residue by vaporizing the solvent. This residue was weighed and recorded as w_1, washed with 5 ml hexane three times to obtain the mass of lipids that are free of solids, while the remaining solids were dried until the weight remained constant and recorded as w_2. The lipid-free solids

weight (w_p) obtained from the biomass was calculated using the following Equation 1.

$$w_p = w_1 - w_2 \quad (1)$$

The extraction yield is the weight of extracted lipids compared to the weight of dry microalgae as indicated in Equation (2).

$$y = \frac{w_p}{w_{mi}} \quad (2)$$

Where, y is extraction yield and w_{mi} is the weight of dry microalgae used as the sample.

2.5 Experimental Procedures

2.5.1. The Extraction Energy Requirement Calculation

The discrete flow system of the HCLE process requires energy to drive the microalgae and solvent to flow through the cavitator in order to generate the cavitation. This energy was calculated by multiplying the air pressure booster with the cross-sectional area of the sample chamber and sample depth using the relationship in Equation (3).

$$E = 9.8P\frac{\pi}{4}D^2L \quad (3)$$

Where, E is the extraction energy required (Joule), P is the pressure of the sample chamber (kg/cm^2), D is the diameter of the sample chamber (cm), L is the distance of the sample surface to the cavitator (cm) and, 9.8 is the conversion factor from kgf to Newton.

2.5.2. Mathematical Model

The HCLE is the process of transferring lipid from the solid (microalgae) to the liquid (solvent) phase using hydrodynamic cavitation and to aid the disruption of the microalgae wall. The inception cavitation number used to generate the cavitation for this system is 0.45 [25] while the Reynold number was more than 32,000, thereby, indicating fully turbulent flow. These values were used because the microalgae have a very small particle size, ranging from 1 to 10 µm [26]. The other assumptions made to govern the model include the following:

a. Diffusion mass transfer in the microalgae body is neglected because of the small size of microalgae cells.
b. Diffusion mass transfer in the fluid film is neglected because there is a turbulent flow in the fluid.
c. The convective mass transfer mechanism is the main process of mass transfer.

It is important to note that two others assumptions were made based on the disrupted and intact types of microalgae cells. The first assumption is that the lipid mass transfer from the disrupted and intact microalgae is taken as the total lipid mass transfer from the microalgae to the solvent and this means only one value of the volumetric mass transfer coefficient represents the lipid mass transfer as illustrated in Figure 2a. The second assumption is that the lipid mass transfer from the disrupted and intact microalgae was obtained separately which led to two different values of volumetric mass transfer coefficient as indicated in Figure 2b. This, therefore, led to the development of two different models based on these assumptions.

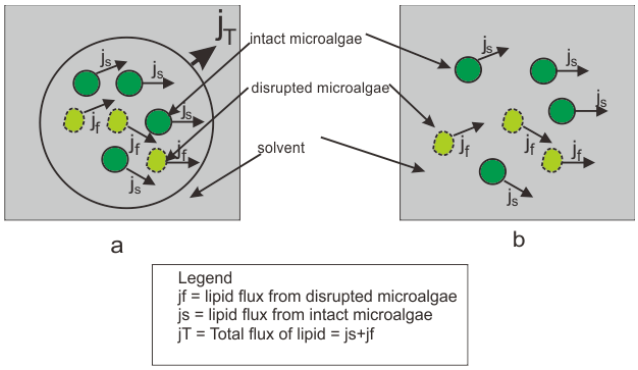

Figure 2. Illustration of Lipid Mass Transfer: a) Total Lipid Mass Transfer and b) Lipid Mass Transfer from Disrupted and Intact Microalgae.

2.5.2.1. Model 1: Total Lipid Mass Transfer Approximation

This model is illustrated in Figure 2a with total lipid flux (j_T). It was discovered at the initial condition of the solid-fluid extraction that the concentration of lipid in the solvent (y) is zero while the changing value of y as a function of the time is equal to the amount of lipids released from the solid (j_T), and this is presented as Equation (4):

$$m_f \frac{\partial y}{dt} = j_T \quad (4)$$

Where, m_f represents the mass of the fluid phase and t represents time. It is also important to note that the amount of lipid released is equal to the mass transfer coefficient multiplied by the concentration gradient

between the microalgae surface and the bulk of liquid which is represented in the following Equation (5):

$$j_T = k_T a_T m_f (y^* - y) \quad (5)$$

Where, $k_T a_T$ is the total volumetric mass transfer coefficient and y^* is lipids concentration on microalgae surface. The value of y^* can be predicted using Equation (6):

$$y^* = K.x \quad (6)$$

2.5.2.2. Model 2. Separately Disrupted and Intact Lipid Mass Transfer Approximation

The lipid mass transfer from the disrupted and intact microalgae was obtained separately in this model and the changing lipid concentration in the solvent is presented as Equation (7):

$$m_f \frac{\partial y}{dt} = j_f + j_s \quad (7)$$

Where, j_f is the lipid mass flux from the disrupted microalgae and j_s is the lipid mass flux from the intact microalgae. Moreover, the lipid mass flux from disrupted microalgae is a function of disrupted microalgae fraction and changing lipid concentration in the microalgae which are represented by the following Equation (8):

$$r m_s \frac{dx_1}{dt} = -j_f \quad (8)$$

Where, r is the fraction of disrupted microalgae, x_1 is the lipid concentration in the disrupted microalgae, and m_s is the mass of dry microalgae. The lipid mass flux from disrupted microalgae can also be written as the mass transfer equation in Equation (9):

$$j_f = k_f a_o m_f (y^*_1 - y) \quad (9)$$

Where, $k_f a_o$ represents the volumetric mass transfer coefficient from disrupted microalgae and y^*_1 is the lipid concentration at the surface of disrupted microalgae. Meanwhile, the lipid mass transfer from intact microalgae is presented as indicated in Equation (10):

$$(1 - r) m_s \frac{dx_2}{dt} = -j_s \quad (10)$$

Where, x_2 represents lipid concentration in the intact microalgae. The lipid mass flux from intact microalgae can also be written as a mass transfer equation as indicated in the following Equation (11):

$$j_s = k_s a_s m_f (y^*_2 - y) \quad (11)$$

Where, $k_s a_s$ represents volumetric mass transfer coefficient from intact microalgae and y^*_2 represents lipid concentration at the surface of intact microalgae.

III RESULTS AND DISCUSSION

3.1. The Extraction Energy Requirement

The results of the extraction energy requirement (E) calculated as a function of repetition number are described in the following Figure 3a.

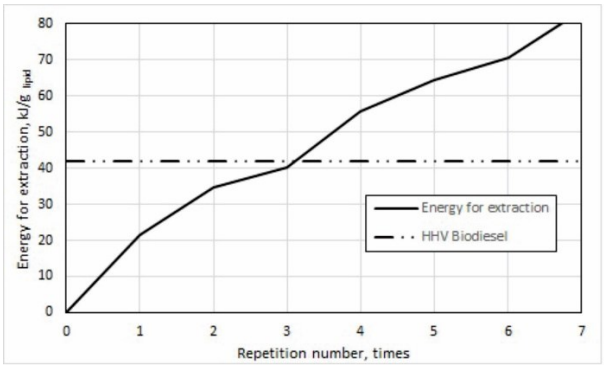

Figure 3a. Extraction energy requirement (E) as a function of the number of repetitions at the pressure of 6.8 kg/cm^2, a temperature of 30°C, and cavitation number of 0.068

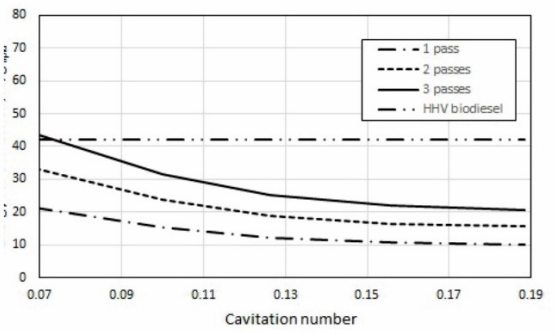

Figure 3b. Extraction energy requirement (E) as a function of the cavitation number at the pressure of 6.8 kg/cm^2 and temperature of 30 °C

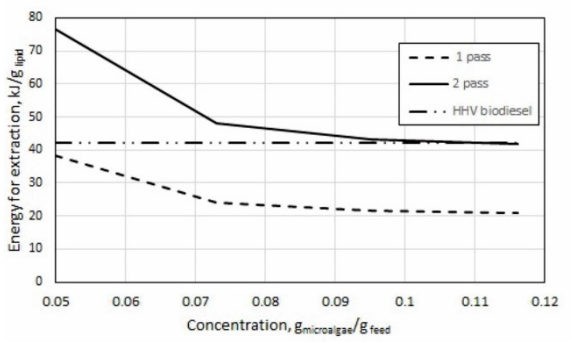

Figure 3c. Extraction energy requirement (E) as a function of the microalgae concentration at the pressure booster of 6.8 kg/cm^2 and the temperature of 30°C

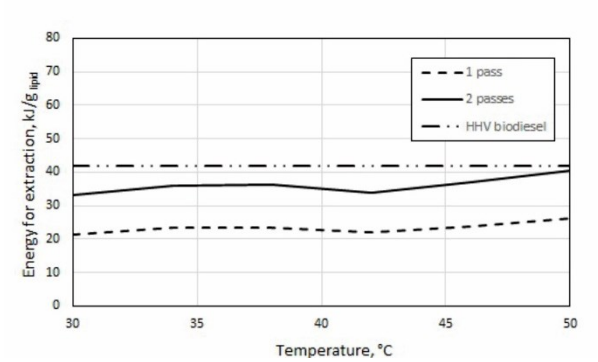

Figure 3d. Extraction energy requirement (E) as a function of the temperature at the pressure booster of 6.8 kg/cm^2 and cavitation number of 0.068

Figure 3a shows that the value of E increased linearly as the number of repetitions increased because the energy used for each extraction step was the same as the constant pressure booster. It was also discovered that this E value was one-third of the HHV of biodiesel which is as high as 42 kJ/g [27] at the condition. Moreover, the influence of the pressure booster on the E value was represented by the effect of cavitation number (σ) on the value and this was calculated using Equation (12) [25].

$$\sigma = \frac{p_2 - p_v}{{}^1/_2 \rho v^2} \quad (12)$$

Where, P_2 is the pressure booster, P_v is the vapor pressure of the fluid, and v is the fluid linear velocity. The E value was subsequently calculated as a function of σ as described in Figure 3b.

Figure 3b shows that the E value tends to decrease as the σ increase and this means the energy requirement is lower at higher σ because the pressure is low. In this case, the HCLE found the limit or maximum value of σ during the process of cavitation and this is called an inception cavitation number (σ_i) with the value observed to depend on the type of the channel such that the σ_i was recorded to be 0.45 when elliptical form with an axis ratio of ¼ was used. Beside this limitation, a higher σ value tends to produce a constant E value and this means the amount of energy input is decreased at higher σ while the constant E value indicates lower yield extraction. This shows the conduct of HCLE at a high σ value is not economical and the best value was obtained at approximately 0.13 when the E value started to become constant.

The microalgae and solvent formed a solid-liquid system with fast settling slurries. It is important to note that the solid concentration slips the velocity in the system [28] and Figure 3c shows that the extraction energy requirement tends to decrease as the microalgae concentration increases. This means the amount of energy input is equal for each concentration with the constant pressure booster. The decreasing E value indicates an increase in the amount of lipid extracted. Meanwhile, the E value tends to be constant at the concentration above 0.073 g microalgae/g feed and this also means the amount of lipid extracted remains constant and this shows a reduction in the yield at high concentration compared to the microalgae feed. Therefore, the optimal concentration in this condition was found to be 0.073 g microalgae/g feed.

The extraction process is affected by temperature [29] as indicated by the decrease in the extraction efficiency when the solid concentration was reduced during the process of extracting Jatropha oil using a mixture of methanol and hexane solvent [30]. Moreover, temperature shows a significant contribution to the distribution coefficient, and this relationship was determined according to the Van't Hoff Equation as follows [31].

$$\ln K = -\frac{\Delta H^o}{RT} + \frac{\Delta S^o}{R} \quad (13)$$

Where, K is the distribution coefficient, ΔH^o is the enthalpy change in the standard condition (kJ/mole), ΔS^o is the entropy change in the standard condition (J/mole/K), and R is the universal gas constant (J/mole/K), and the value of ΔH^o and ΔS^o in the common extraction process are both positive [31].

A previous study conducted by the authors showed that the value of K was influenced by temperature such that an increase in the temperature lead to an increase in the K values [21]. Meanwhile, the effect of temperature on extraction energy requirement in the HCLE process is described in Figure 3d which shows that the E value slightly increased from 30 to 37°C followed by a decrease to 42°C and a later increase. Moreover, the minimum energy requirement was found to be 21.464 kJ/kg lipid for 1 pass extraction at 30°C and this means this is the optimum temperature for the process.

3.2. Lipid Release Mechanism

Microalgae lipids are entrapped and protected by cell walls which need to be disrupted to ensure an efficient lipid extraction from the matrix using a solvent. The understanding of the mechanism of lipids released from microalgae in the HCLE is an important step to making the right assumptions in the mass transfer model evaluation. The difference between the lipids release rate from the disrupted and intact microalgae needs to be determined to understand this mechanism. Therefore, this study compared the HCLE and conventional extraction techniques, and the results presented in Figure 2 showed that the yield of the HCLE was higher than the conventional process, thereby, indicating the lipid release in the HCLE was not only from the intact but also from the disrupted microalgae [32]. This is possible because the method is assumed to involve a simultaneous extraction of lipid from disruption and intact microalgae while the conventional method is only from the intact microalgae [23].

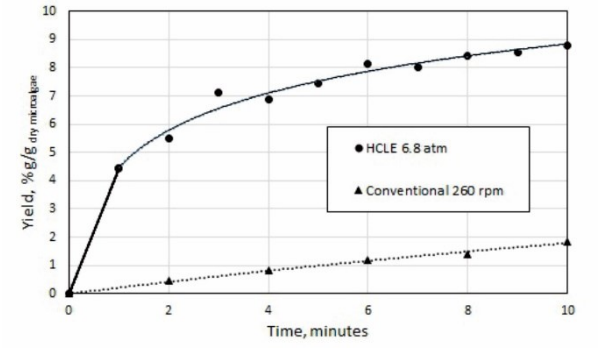

Figure 4a. Comparison of extraction curve between HCLE and conventional extraction

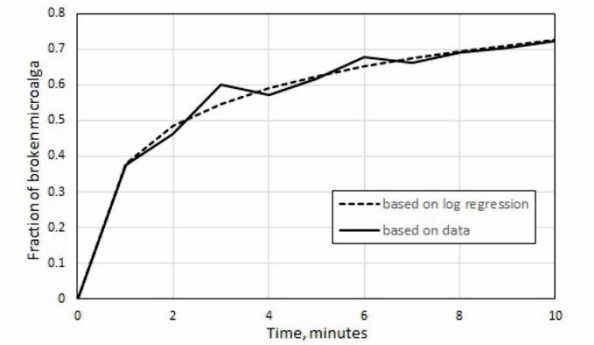

Figure 4b. Fraction of disrupted microalgae as a function of time

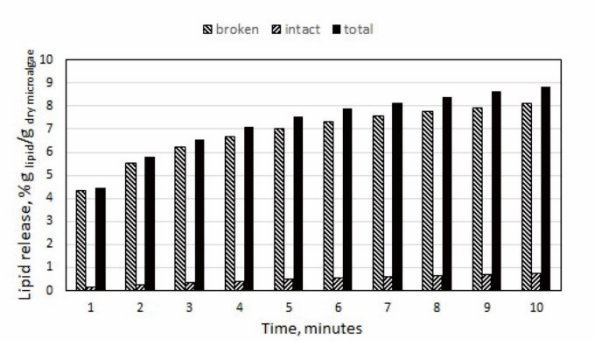

Figure 4c. Comparison of lipids released from disrupted and intact microalgae

Figure 4a shows that the extraction rate using HCLE was higher compared to the conventional technique. It was also discovered that the HCLE showed three different zones with the extraction curve divided into two or three sections [33] while the conventional extraction tends to change linearly during the time interval. The biggest difference between the two processes was observed at the initial process with the HCLE rate found to be faster and this indicates the extraction at the section was determined by the lipid released by disrupting microalgae. In the second section which was from the second to the fifth minute, the rate decreased but was also higher than the conventional technique while after 5 minutes, which is the third section, the rate was equal for both processes. This simply shows that the lipid mass transfer is determined by the intact cell while the transfer in the first section of the HCLE was assumed to be only from the disrupted microalgae to fluid with the intact microalgae neglected because its rate was very small compared to the disrupted. Moreover, the lipid concentration in the disrupted microalgae after the extraction process was equal to the equilibrium value because it was effectively washed with methanol and hexane solvent [34].

3.3. Evaluation of Microalgae Cell Disruption

Microalgae cell disruption can be assessed by measuring intracellular components such as the extracted lipids [34] while the portion of cell disruption in the HCLE can be predicted using lipid mass balance. This is possible because the total lipids in the solvent are released from the disrupted and intact microalgae as indicated in Equation (14).

$$y = rm_s(x_0 - x_e) + (1 - r)m_s y_c \quad (14)$$

Where, x_0 is the initial lipid concentration in the microalgae and the value is different for each repetition of extraction, x_e is lipid concentration in the disrupted microalgae, and y_c is lipid concentration extracted using the conventional method. The value of x_0 can be written as Equation (15).

$$x_{0,i+1} = x_{0,i} - y_{c,i} \quad (15)$$

Where, i is the time dimension or number of repetitions. Meanwhile, y_c can be solved empirically using Ms. Excel based on the conventional extraction data in Figure 4a as indicated in the following Equation (16).

$$y_c = -0.0031t^2 + 0.2154t \quad (16)$$

Where, t is the extraction time. The fraction of disrupted microalgae (r) can also be calculated based on y data and y_c in Figure 3 using Equation (14) by iteration methods. The r calculated for each time is presented in Figure 4b.

Figure 4b shows that the cell disruption trend was similar to the HCLE lipid yields presented in Figure 4a and this means the amount of lipids released from the microalgae to the solvent in the HCLE was determined by the microalgae cell disruption. Moreover, the fraction of cell disrupted was used to determine the amount of lipids released from the disrupted and intact microalgae as shown in Figure 4c. It was discovered that the amount of lipids released from the disrupted microalgae is more than for intact microalgae, especially at the beginning of the process, while the fraction released from the intact microalgae tends to increase along the process due to the reduction in the degree of disruption.

3.4. The HLCE Fitting Models

3.4.1. *Total Lipid Mass Transfer Model (Model 1)*

The HCLE total lipid mass transfer model (Model 1, Equation 4) was numerically solved using the Runge-Kutta method while the value of the volumetric mass transfer coefficient ($k_T a_T$) was evaluated using the Golden Section method for one variable minimization with the minimum target of the sum of square of errors (SSE) which was formulated as shown in Equation (17).

$$SSE = \sum(y_{calc} - y_{data})^2 \quad (17)$$

Where, y_{calc} is the value of y calculated from Equation (4) and y_{data} is the value of y from the experiment. There are two estimations in solving this model and the first involves using one section of the extraction curve to have only one value of $k_T a_T$ for the whole time while the second focuses on using three sections of extraction curves to have three different values of $k_T a_T$ for each section. The results for the model are described in Figure 5a.

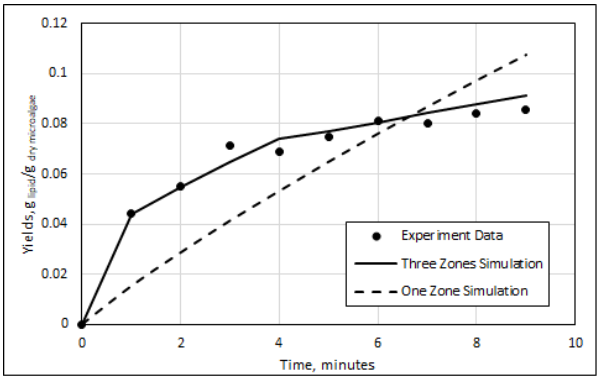

Figure 5a. Model plotting with an assumption of total flux mass

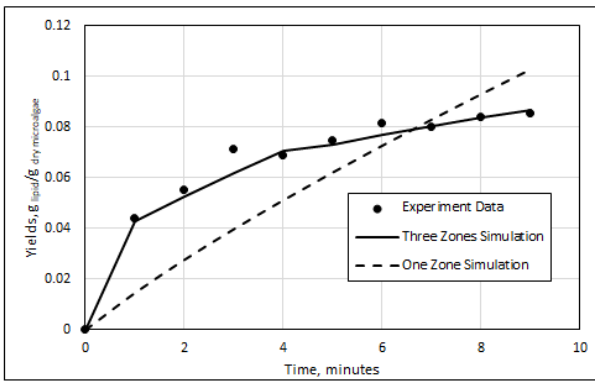

Figure 5b. Model plotting with the assumption from disrupted and intact microalgae flux mass.

3.4.1.1. Model Solution Using One Section

Figure 5a shows that the approximation using one section or one value of $k_T a_T$ provided an almost linear simulation result. The application of the assumptions of a single value of $k_T a_T$ was observed to provide a linear relationship between yield function and time because the amount of lipids released from the disrupted and intact microalgae for each step was calculated using the lipid concentration in the microalgae as the conventional extraction. This led to the lipid concentration difference in the microalgae and the solid because the lipid mass transfer driving force was not significantly different for each step.

The value of $k_T a_T$ was 0.6087 1/minute while the coefficient of determination value was 0.4347 and this generally means the approximation was very bad and unable to be effectively used to describe the HLCE.

3.4.1.2. Model Solution Using Three Sections

The approximation of the extraction curve using three sections was conducted by dividing the extraction process based on the value of the curve slope [33]. The value of $k_T a_T$ in this method is tabulated in Table 1.

Table 1. Value of Volumetric Mass Transfer of HCLE

One Section Approximation			Three Sections Approximation			
Time, minutes	$k_T a_T$, 1/minute	R^2	Time, minutes	Section	$k_T a_T$, 1/minute	R^2
1	0,6087	0.4347	1	1	1.7579	0.9783
2			2			
3			3	2	0.4652	
4			4			
5			5			
6			6			
7			7			
8			8	3	0.1925	
9			9			
10			10			

Figure 5a shows that the first section, which is the beginning of the extraction process from 0 to 1 minute, produced the highest extraction rate as indicated by the highest curve slope value of 0.04423. The second section was the middle extraction rate from 1st to 5th minute with a slope value of 0.00745 and the third section was at the constant extraction rate from the 6th minute to the end of the process with a slope value of 0.00239. Table 1 shows that the extraction using this three-section approximation produced a better result than one section with the R^2 value of 0.9783 and this means it has the ability to describe the HCLE process effectively. This indicates the existence of three values of $k_T a_T$ differentiated by the a_T values associated with the cell disruption.

3.4.1.3. *Separated Lipid Mass Transfer from Disrupted and Intact Microalgae Model (Model 2)*

The volumetric mass transfer from the disrupted microalgae ($k_f a_o$) and intact microalgae ($k_s a_s$) was separately evaluated in this model using two approximations of single and three sections. The results are presented in Figure 5b.

3.4.2.1. Model Solution Using One Section

Figure 5b shows that the approximation using one section or one value of $k_f a_o$ and $k_s a_s$ produced a better simulation than Model 1 as indicated by 0.5835 and 0.030 1/minutes respectively with the coefficient of determination value recorded to be 0.4415. This approximation has a large deviation and this means it cannot be used to describe the HLCE process.

3.4.2.2. Model Solution Using Three Sections

The extraction curve was divided into three sections based on the difference in the value of the slopes. The first section, from minute 0 to 1, was the beginning extraction process and had the highest extraction rate as indicated by the highest curve slope value of 0.04423. The second section was the middle extraction rate, from minute 1 to 4, with a slope value of 0.00824 and the third section, from minute 5 to the end of the process, had a constant extraction rate with a slope value of 0.00318. The values of $k_f a_o$ and $k_s a_s$ using this approximation are presented in Table 2.

Table 2. Value of $k_f a_o$ and $k_s a_s$ and R^2 from Model 2

1 Section				3 Sections			
Time, minutes	$k_f a_o$	$k_s a_s$	R^2	Time, minutes	$k_f a_o$	$k_s a_s$	R^2
1				1	1.708	0.051	
2				2	0.436	0.030	
3				3	5		
4	0.5835	0.030	0.4415	4			0.9778
5				5			
6				6			
7				7	0.1829	0.011	
8				8			
9				9			
10				10			

Table 2 shows that the approximation using 3 sections of extraction provided the best result for the two models with Model 2 observed to be better than Model 1 and this means it has the ability to describe the HCLE process better.

3.5. Comparison between Model 1 and Model 2

The calculation of the disrupted and intact microalgae approximation separately showed that Model 1 and 2 have equal results with R^2 values of 0.9783 and 0.9778 respectively and this means they can both be used to describe the HCLE process because the percentage of lipid released from the intact microalgae is too small compared to the disrupted. The most significant difference was found at the beginning of the process such that the percentage of lipid released from the intact microalgae at minute-1 (1 pass) extraction was 2.95% while the disrupted microalgae had 97.05%. These values changed with time as observed with an increase in the intact microalgae while disrupted microalgae decreased such that the percentage of lipid released at the 10th minute (10 passes) was 8.36% and 91.64% respectively. It is important to note that the HCLE process was determined early at the 5th minute when 85% of total lipids had been extracted. This means a simpler approximation involving total lipid released can be used to describe the process considering the fact that the intact microalgae only produced a small percentage of lipid.

IV CONCLUSION

The extraction energy requirement (E) for HCLE using a discrete flow system was observed to be influenced by the number of repetitions, cavitation number, microalgae concentration, and temperature process. The value can be adjusted to ensure it is lower than the HHV of biodiesel by setting these variables. It was also discovered that the lowest E value was 10 kJ/gram lipid and this means the process is promising to be developed and scaled up for commercial applications.

The HCLE was also modeled using different mass transfer models including the total mass transfer from intact and disrupted microalgae (Model 1) and separated mass transfer (Model 2) using both one and three sections of the extraction curve. The results showed that both models provided the same result due to the very small amount of lipid released from the intact microalgae compared to the disrupted microalgae. Moreover, the volumetric mass transfer coefficient value decreased from sections 1 to 3. In the case of HCLE with Model 1, the $k_T a_T$ value for sections 1, 2, and 3 were 1.7579, 0.4652, and 0.1925 1/min respectively with a coefficient of determination (R^2) of 0.9783 while the $k_f a_o$ values for Model 2 were 1.708, 0.4365, and 0.1829 1/min and $k_s a_s$ were 0.051, 0.030 and 0.011 1/min respectively with an R^2 value of 0.9778.

Acknowledgments

The authors appreciate the Process System Engineering Research Group, Chemical Engineering Department, Gadjah Mada University, Yogyakarta, Indonesia for providing the research facilities and Ahmad Dahlan University, Yogyakarta, Indonesia for assisting with the research fund.

References

[1] Y. S. Pradana, H. Sudibyo, E. A. Suyono, Indarto, and A. Budiman, "Oil algae extraction of selected microalgae species grown in monoculture and mixed cultures for biodiesel production," *Energy Procedia*, vol. 105, pp. 277–282, 2017.

[2] H. Sudibyo, Y. S. Pradana, T. T. Samudra, A. Budiman, Indarto, and E. A. Suyono, "Study of cultivation under different colors of light and growth kinetic study of Chlorella zofingiensis Dönz for biofuel production," *Energy Procedia*, vol. 105, pp. 270–276, 2017.

[3] T. M. Mata, A. A. Martins, and N. S. Caetano,

"Microalgae for biodiesel production and other applications: A review," *Renew. Sustain. Energy Rev.*, vol. 14, no. 1, pp. 217–232, 2010.

[4] J. P. Maity, J. Bundschuh, C. Y. Chen, and P. Bhattacharya, "Microalgae for third generation biofuel production, mitigation ofgreenhouse gas emissions and wastewater treatment: Present andfuture perspectives - A mini review," *Energy*, vol. 78, pp. 104–113, 2014.

[5] T. Suganya, M. Varman, H. H. Masjuki, and S. Renganathan, "Macroalgae and microalgae as a potential source for commercial applications along with biofuels production: A biorefinery approach," *Renew. Sustain. Energy Rev.*, vol. 55, pp. 909–941, 2016.

[6] Sunarno, Rochmadi, P. Mulyono, M. Aziz, and A. Budiman, "Kinetic study of catalytic cracking of bio-oil over silica-alumina catalyst," *BioResources*, vol. 13, no. 1, pp. 1917–1929, 2018.

[7] D. R. Sawitri, Sutijan, and A. Budiman, "Kinetics study of free fatty acids esterification for biodiesel production from palm fatty acid distillate catalysed by sulphated zirconia," *ARPN J. Eng. Appl. Sci.*, vol. 11, no. 16, pp. 9951–9957, 2016.

[8] S. Kathirvel, A. Layek, and S. Muthuraman, "Engineering Science and Technology , an International Journal Exploration of waste cooking oil methyl esters (WCOME) as fuel in compression ignition engines : A critical review," *Eng. Sci. Technol. an Int. J.*, vol. 19, no. 2, pp. 1018–1026, 2016.

[9] Daniyanto, Sutijan, Deendarlianto, and A. Budiman, "Reaction kinetic of pyrolysis in mechanism of pyrolysis gasification process of dry torrified sugarcane bagasse," *ARPN J. Eng. Appl. Sci.*, vol. 11, no. 16, pp. 9974–9980, 2016.

[10] D. R. Wicakso, Sutijan, Rochmadi, and A. Budiman, "Study of Catalytic Upgrading of Biomass Tars using Indonesian Iron Ore," in *AIP Conference Proceedings*, 2017, vol. 20094, pp. 1–8.

[11] S. Jamilatun, A. Budiman, Budhijanto, and Rochmadi, "Non-catalytic slow pyrolysis of Spirulina Platensis residue for production of liquid biofuel," *Int. J. Renew. ENERGY Res. S. Jamilatun al*, vol. 7, no. 4, 2017.

[12] R. D. Kusumaningtyas, I. N. Aji, H. Hadiyanto, and A. Budiman, "Application of tin (II) chloride catalyst for high FFA Jatropha oil esterification in continuous reactive distillation column," *Bull. Chem. React. Eng. Catal.*, vol. 11, no. 1, p. 66, 2016.

[13] T. Chatsungnoen and Y. Chisti, "Oil production by six microalgae: impact of flocculants and drying on oil recovery from the biomass," *J. Appl. Phycol.*, vol. 28, no. 5, pp. 2697–2705, 2016.

[14] P. Collet *et al.*, "Biodiesel from microalgae–Life cycle assessment and recommendations for potential improvements," *Renew. Energy*, vol. 71, pp. 525–533, 2014.

[15] E. Suali and R. Sarbatly, "Conversion of microalgae to biofuel," *Renew. Sustain. Energy Rev.*, vol. 16, no. 6, pp. 4316–4342, 2012.

[16] A. K. Lee, D. M. Lewis, and P. J. Ashman, "Force and energy requirement for microalgal cell disruption: An atomic force microscope evaluation," *Bioresour. Technol.*, vol. 128, pp. 199–206, 2013.

[17] A. K. Lee, D. M. Lewis, and P. J. Ashman, "Microalgal cell disruption by hydrodynamic cavitation for the production of biofuels," *J. Appl. Phycol.*, vol. 27, no. 5, pp. 1881–1889, 2015.

[18] K. de Boer, N. R. Moheimani, M. A. Borowitzka, and P. A. Bahri, "Extraction and conversion pathways for microalgae to biodiesel: A review focused on energy consumption," *J. Appl. Phycol.*, vol. 24, no. 6, pp. 1681–1698, 2012.

[19] B. Momin, S. Chakraborty, and U. Annapure, "Investigation of the cell disruption methods for maximizing the extraction of arginase from mutant Bacillus licheniformis (M09) using statistical approach," *Korean J. Chem. Eng.*, vol. 35, no. 3, pp. 1–12, 2018.

[20] H. Yen, I. Hu, C. Chen, S. Ho, D. Lee, and J. Chang, "Microalgae-based biorefinery – From biofuels to natural products," *Bioresour. Technol.*, vol. 135, pp. 166–174, 2013.

[21] M. Setyawan, P. Mulyono, Sutijan, and A. Budiman, "Comparison of Nannochloropsis sp . cells disruption between hydrodynamic cavitation and conventional extraction," in *MATEC Web of Conferences*, 2018, vol. 1023, pp. 1–5.

[22] S. I. Choi, J. P. Feng, H. S. Seo, Y. M. Jo, and H. C. Lee, "Evaluation of the cavitation effect on liquid fuel atomization by numerical simulation," *Korean J. Chem. Eng.*, vol. 35, no. 11, pp. 2164–2171, 2018.

[23] I. Lee and J. I. Han, "Simultaneous treatment (cell disruption and lipid extraction) of wet microalgae using hydrodynamic cavitation for enhancing the lipid yield," *Bioresour. Technol.*, vol. 186, pp. 246–251, 2015.

[24] L. Paulo, S. Silva, and J. Martínez, "Mathematical modeling of mass transfer in supercritical fluid extraction of oleoresin from red pepper," *J. Food Eng.*, vol. 133, pp. 30–39, 2014.

[25] J.-P. Franc and J.-M. Michel, *Fundamentals of Cavitation*. New York: Kluwer Academic Publishers, 2005.

[26] T. A. Beacham, C. Bradley, D. A. White, P. Bond, and S. T. Ali, "Lipid productivity and cell wall ultrastructure of six strains of Nannochloropsis: Implications for biofuel production and downstream processing," *Algal Res.*, vol. 6, no. PA, pp. 64–69, 2014.

[27] K. Sivaramakrishnan and P. Ravikumar, "Determination of Higher Heating Value of Biodiesels," *Int. J. Eng. Sci. Technol.*, vol. 3, no. 11, pp. 7981–7987, 2011.

[28] R. H. Perry and D. W. Green, "10. Transport and storage of fluids," in *Perry's Chemical Engineers' Handbook*, 2008, p. 2400.

[29] M. A. Islam, R. J. Brown, I. O'Hara, M. Kent, and K. Heimann, "Effect of temperature and moisture on high pressure lipid/oil extraction from microalgae," *Energy Convers. Manag.*, vol. 88, pp. 307–316, 2014.

[30] Y. He *et al.*, "Nontoxic oil preparation from Jatropha curcas L. seeds by an optimized methanol/n-hexane sequential extraction method," *Ind. Crops Prod.*, vol. 97, pp. 308–315, 2017.

[31] J. L. A. Dagostin, D. Carpiné, and M. L. Corazza, "Extraction of soybean oil using ethanol and mixtures with alkyl esters (biodiesel) as co-solvent: Kinetics and thermodynamics," *Ind. Crops Prod.*, vol. 74, pp. 69–75, 2015.

[32] K. Yamamoto, P. M. King, X. Wu, T. J. Mason, and E. M. Joyce, "Effect of ultrasonic frequency and power on the disruption of algal cells," *Ultrason. Sonochem.*, vol. 24, pp. 165–171, 2015.

[33] H. Sovová, "Mathematical model for supercritical fluid extraction of natural products and extraction curve evaluation," *J. Supercrit. Fluids*, vol. 33, no. 1, pp. 35–52, 2005.

[34] J. A. Gerde, M. Montalbo-Lomboy, L. Yao, D. Grewell, and T. Wang, "Evaluation of microalgae cell disruption by ultrasonic treatment," *Bioresour. Technol.*, vol. 125, pp. 175–181, 2012.

FREE 1 (2022) 13-22

Frontiers in Renewable Energy (FREE)

Journal homepage: www. https://jurnal.ugm.ac.id/v3/FREE/

Sub-Regimes of Air-Water Slug Flow Characteristics in Horizontal Pipes by Liquid Hold-up Model Correlated to Bubble Behaviors (LHmBb)

Yosephus Ardean Kurnianto Prayitno [1,2*], Okto Dinaryanto[3], Deendarlianto[2,4], and Indarto[4]

[1] of Mechanical Engineering, Vocational College, Universitas Gadjah Mada, Sekip Unit 1, Bulaksumur, Yogyakarta, 55281, Indonesia
[2] Center for Energy Studies, Universitas Gadjah Mada, Sekip K-1A, Bulaksumur, Yogyakarta, 55281, Indonesia
[3] Department of Mechanical Engineering, Faculty of Aerospace Technology, Institut Teknologi Dirgantara Adisutjipto, Blok R Lanud Adisutjipto, Yogyakarta 55198, Indonesia
[4] Department of Mechanical and Industrial Engineering, Faculty of Engineering, Universitas Gadjah Mada, Jalan Grafika No.2, Bulaksumur, Yogyakarta, 55281, Indonesia

ARTICLE INFO

Article history:
Received 27 November 2021
Revised 1 December 2021
Accepted 1 March 2022
Available online 10 August 2022

Key words:
sub-regime, slug flow, horizontal pipe, liquid hold-up, bubble behaviors

ABSTRACT

The air-water slug flow sub regimes in horizontal pipes were characterized by a liquid hold-up model correlated to bubble behavior (LHmBb). The LHmBB has two sections, the liquid hold-up model and bubble behavior investigations. The liquid hold-up model was developed based on the statistical analysis of the probability density function (PDF) to quantify the bubble distribution. Specifically, the distribution was qualitatively investigated based on the high-speed camera and correlated to the quantified LH to characterize the sub-regime of air-water slug flow. The LHmBB characterized the air-water slug flow sub-regimes in a horizontal transparent acrylic pipe with an inner diameter of Ø= 0.026 m under air and water superficial velocities of $J_G = 0.31 - 6.00$ m/s $J_L = 0.20 - 0.44$ m/s, respectively. As a result, four sub-regimes were determined as Initially dispersed Bubbles (IdB), Low dispersed Bubbles (LdB), High dispersed Bubbles (HdB), and Dominantly dispersed Bubbles (DdB). The decreasing number of bubbles and dispersing bubbles mechanism determined the type of sub-regime. The proposed LHmBb included the correlation function to ease the prediction of the sub-regimes of air-water slug flow characteristics, leading to the two-phase flow pattern map in horizontal pipes enhancement.

2.1. INTRODUCTION

In industrial applications, air-water two-phase flow inside the pipes occurs in various ways. For instance, during the transition stages, growing waves in the oil and gas refinery piping system generate high oscillatory pressure. This leads to high vibrations on the piping structure, causing cracking and corrosion [1]. The

Peer review under responsibility of Frontiers in Renewable Energy (FREE).
*Corresponding author.
E-mail address: yosephus.ardean@ugm.ac.id (Yosephus Ardean Kurnianto Prayitno)
0001-00012/ 2022. Published by Frontiers in Renewable energy (FREE).

transition stages covering the initiation through the intermittent to the developed flow were characterized by the air-water two-phase flow inside the pipes, valuable for minimizing the damage in the pipes. Previous studies focused on understanding the complex characteristics of the developed flow, including limited works on the initiation and the intermittent flow. In our previous studies, the initiation and development flow were experimentally investigated in a horizontal pipe resulting in several basic characteristics of slug flow initiation evaluated by slug initiation and the passing slug frequency [2]. Arabi et al. investigated the slug flow characteristic in the intermittent flow by its frequency with an empirical correlation to the experimental data based on the liquid volume fraction, to respond to the initiation flow characteristics [3]. Therefore, a deep understanding of the sub-regime of air-water slug flow characteristics inside the pipes helps prevent the drawbacks in the industrial pipelines.

The characteristics of air-water slug flow sub regimes were proposed by several related studies. The characteristics include Kelvin-Helmholtz (KH) instability of a stratified flow, viscous linear instability of a stratified flow by long is long-wavelength (VLW), and stability of a slug flow [4]. The KH instability explained that the mechanism of wave growth for inviscid fluid is not feasible for predicting the actual sub-regimes of air-water slug flow characteristics because the fluid has no viscosity [5]. The VLW instability is also known as Viscous Kelvin-Helmholtz (VKH), which provides a better prediction. The VLW instability is analyzed based on the growth of small amplitude, long wavelength disturbances and shear stresses, and destabilizing effects of liquid inertia. However, the VLW instability is difficult to be observed for sub-regime of air-water slug flow characteristics [6]. The VLW instability was upgraded by Hurlburt and Hanratty [7] in terms of stability compared to the slug stability theory proposed by Taitel and Dukler [5]. This was achieved by determining the relationship between the bubble velocity and the mixture velocity to estimate the critical height of the liquid layer. Based on the above studies, the details investigation of bubble parameters is important for characterizing the sub-regimes of air-water slug flow.

In order to investigate the details of bubble parameters, several previous works by means of liquid hold-up model were reported. Conventionally, an electrical impedance was used to measure the experimental liquid hold-up with respect to the threshold value to determine the flow regime [8]. On the other hand, a constant-electrical-current method (CECM) was used to determine the time varying thickness of liquid film flowing with high-speed gas flow [9]. Up to now, vast improvement on liquid hold-up model is introduced to provide more comprehensive analysis compared to the conventional one. In our previous research, the air-water slug flow sub regimes were characterized in 16 mm horizontal pipe based on the experimental liquid hold-up and pressure fluctuations [10]. The simplified correlation was proposed for vast prediction of experimental liquid hold-up in annular flow as comprehensive analysis [11]. Since the liquid hold-up covers the complex characteristics in a wide range of flow regimes, a correlation model to bubble behavior is considered.

In order to comprehensively characterize the air-water slug flow sub regimes in horizontal pipes, a liquid hold-up model correlated to bubble behaviors (LHmBb) was proposed. This study aimed to 1) quantify the bubble behaviors in sub-regimes of air-water slug flow, 2) determine the characteristics of sub-regimes air-water slug flow by LHmBb, and 3) develop a correlation function based on LHmBb for the prediction model of the characteristics of sub-regimes air-water slug flow. This work is dedicated to support the theoretical model development and validation of CFD codes [12], [13] by high-quality temporal and spatial experimental data of air-water slug flow sub-regimes. Moreover, the proposed model is valuable for the development of advanced machine learning for two-phase flow application, such as a comprehensive input model in plural long short-time memory with sparse model implemented in multiple current-voltage system (pLSTM-SM-MCV) [14].

2.2. LIQUID HOLD-UP MODEL CORRELATED TO BUBBLE BEHAVIOURS(LHmBb)

2.1 Overview

The liquid hold-up model was developed based on the statistical analysis of probability density function (PDF) to quantify the bubble distribution. The bubble

behaviors are qualitatively investigated based on the high-speed camera and correlated to the quantified LH to characterize the air-water slug flow sub-regimes.

2.2 Liquid hold-up model

The fundamental equation of the constant-electric-current-method (CECM) proposed by [9] defined the liquid hold-up model (LHm) where the electric resistance of two-phase flow R_TP in a unit length of the horizontal pipe is expressed as,

$$\frac{1}{R_{TP}} = \frac{1-\alpha}{R_G} + \frac{\alpha}{R_L} \quad (1)$$

Where R_G is the gas resistance, R_L liquid resistance, and α liquid hold-up. Both R_G and R_L represent the electric resistance when the gas and liquid phases occupy the horizontal pipe's whole cross-section. In the case of $R_G \gg R_L$, Eq. (1) can be defined as relating to the voltage drop V_{TP} and injected constant current I as,

$$\alpha = \frac{IR_L}{IR_{TP}} = \frac{V_L}{V_{TP}} \quad (2)$$

Since the voltage drop V_L refers to the case of liquids occupies the whole horizontal pipe's cross-section while flowing, the electric resistance R_{TP}^{ref} and voltage drop V_{TP}^{ref} of two-phase flow with the reference liquid hold-up α^{ref} can be defined by firstly modifying Eq. (2) with respect to I and secondly eliminating V_L as,

$$\alpha^{ref} = \frac{IR_L}{IR_{TP}^{ref}} = \frac{V_L}{V_{TP}^{ref}} \quad (3)$$

$$\alpha = \frac{IR_{TP}^{ref}}{IR_{TP}}\alpha^{ref} = \frac{V_{TP}^{ref}}{V_{TP}}\alpha^{ref} \quad (4)$$

Therefore, the α of the air-water two-phase flow in the horizontal pipe in Eq. (4) can be determined.

2.3 Quantified bubble behaviors

The bubble behaviors β are quantified based on the normalized number of bubbles $\beta_н$, that occupies the whole section of the horizontal pipe during the air-water slug flow. Here, κ is the air-water slug flow patterns which corresponds to the superficial velocity of gas J_G and liquid J_L, respectively. The $\beta_н$ is normalized by the number of bubbles β^{ref}, corresponding to their momentum in air-water two-phase flow. β^{ref} is the maximum value of the air-water two-phase flow's voltage drop V_{TP} in Eq. (4) under specific κ. According to the normalization the technique used by [15], which quantifies the two-phase sludge thickness in centrifugal fields, β can be defined as,

$$\beta = \frac{\beta_к - \beta_к^{ref}}{\beta_к^{ref}} \quad (5)$$

To solve Eq. (6), image processing techniques (IPT) which has been applied in our previous works [16], [17] is referred to quantify the bubble behaviors captured by high-speed camera. The IPT assessed the area of bubble data, equivalent diameter, and perimeter in case of a break-up, traveled, detached/coincided, and dispersed bubble. An active morphological contour without edges (MACwE) technique was used for processing images with visible contours inthe condition of noisy, cluttered, or partially unclear images. The three main steps of MACwE are; 1) thresholding and shading, 2) segmentation and 3) binarization and evolutions. The $\beta_н$ was obtained from the three iterations category denoted as a, b, and c, which represented the area of the bubbles under κ. Where β is from the known $\beta^{ref}$of the whole binary numbers under κ.

$$\alpha' = \frac{V_{TP}^{ref}}{\beta V_{TP}}\alpha^{ref} \quad (6)$$

Thus, the quantitative LHmBb From Eq. (6) is evaluated by the probability density function (PDF), denoted as P as follows,

$$P(\alpha^0 \le \alpha' \le \alpha^m) = \int_{\alpha^0}^{\alpha^m} f_{\alpha'}(\alpha)d\alpha \quad (7)$$

Where α^0 and α^m are the lowest and highest liquid hold-up, respectively, can be measured in the whole section of liquid hold-up.

2.4 Correlation model

In order to correlate the LHm for sub-regime of air-water slug flow characteristics, the quantified bubble behaviors β in Eq. (5), with respect to LHm in Eq. (4), is defined as,

$$\alpha' = \frac{V_{TP}^{ref}}{\beta V_{TP}}\alpha^{ref} \quad (6)$$

III EXPERIMENTS

3.1. Experimental setup

The experiments were carried out at Horizontal Two-Phase Flow Facility (HORTOFF)-Fluid Mechanics Laboratory, Department of Mechanical and Industrial Engineering, Faculty of Engineering, Gadjah Mada University, Indonesia. **Figure 1** shows the experimental setup consisting of an inlet, test, and outlet sections. The inlet section configured the air-water mixer installed to

keep the air and the water flow separately into the test section. The air and water were from the top and bottom sections of the mixer, respectively. For the initial flow alignment and modification of the two-phase flow into a stratified one, a splitter plate was installed at the center of the air-watermixer, as used by Ujang et al. [19] from the former experiments [2], [13], [16], [18]. The test section was composed of a horizontal pipe with a 9 m length and an inner pipe diameter of 0.026 m. The length of the test section is designed for 0-210 of diameter (0-210D) or around 5.46 m to guarantee a stable development of air-water slug flow. The use of the same materials on the entire experimental pipe ensured uniform roughness of the wall. In the outlet section, the ends of the horizontal pipe and each flange were machined to give and maintain smooth junctions and pipes and minimize the gaps.

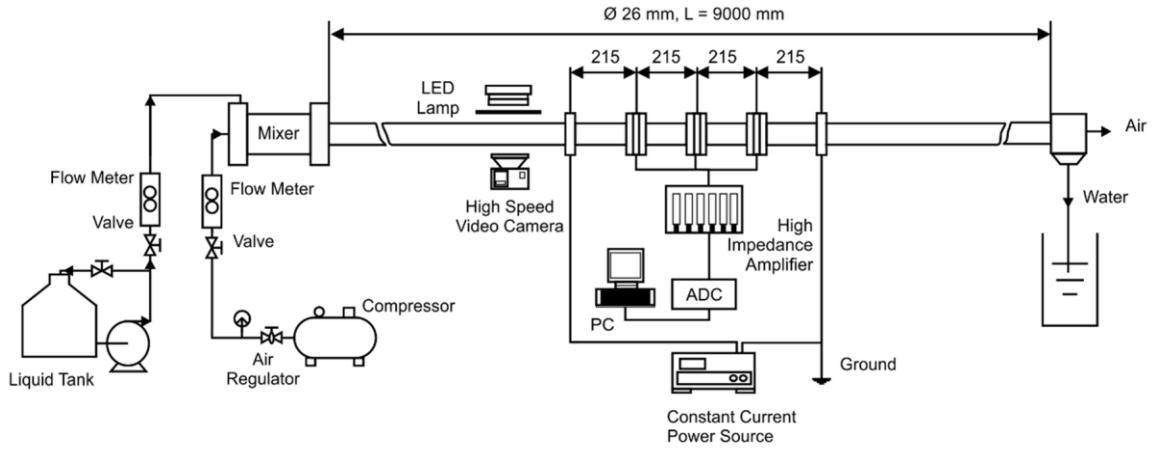

Figure 1. Schematic diagram of the experimental setup.

A room temperature and an atmospheric pressure were maintained during the experiment. On the inlet section, air pressure of 8 bars (gauge) was supplied by a compressor and a maximum amount of 600 LPM. A centrifugal pump with minimum fluctuations compared to other pumps, with a capacity of 18 m^3/h, pumped the water into the section. The installation of a flexible hose on the inlet section rig reduces the flow oscillations and vibrations. To control the flow rate, two types of flow meters were used, namely 1) Dwyer's gas flow meters with capacities range of 1-600 SCFH and 300-1,800 SCFH, and a 3% accuracy and 2) Omega water flow meters with maximum capacity of 10 GPM and an approximate 2% accuracy.

A constant-electric-current method (CECM) with three parallel sensors located at a 215 mm distance was used to obtain the liquid hold up defined in Eq. (6). Bubble behaviors were observed within 120 seconds, focusing on a specific point before the developed flow's measurement points. A high-speed video camera, Phantom Miro-M310, with a maximum frame rate of 1,200 fps and a resolution of 3,000 x 4,000 pixels, was installed at 150D, obtaining the spatial results of visualization studies. The lighting equipment had a series of installed LED lamps on the test section rig. Regarding the distortion from the horizontal pipe, a correction box was installed in the test section pipe, about 5 m from the inlet section. The box reduced image distortion and minimized the difference in refractive indices between the fluids and tube wall [20]. It was made of a rectangular transparentacrylic box filled with water with a refractive index. Therefore, the quality of visualization data could be highly-maintained. The phenomenon in the near-wall was magnified for a better investigation of sub-regime of air-water slug flow characteristics.

3.2. Experimental method and condition

The experimental matrix had a range of air and water superficial velocities as $J_G = 0.31 - 6.00$ m/s and $J_L = 0.20 - 0.44$ m/s. The low-liquid superficial velocities observations were conducted to investigate the transition phenomenon in the presence of the bubbles. At the higher liquid superficial velocities, the focus was on the presence of bubble under the wave

coalescence, the pipe blockage due to wave growth, turbulence penetration, and its relationto the sub-regime phenomenon. Under the high liquid, superficial velocities were to investigate the presence of bubbles pressured by the irregular waves and the initiation positionsof the slug flow. The experimental data were obtained in two stages carried out simultaneously. a) the visualization observation for quantifying the bubble behaviors and b) liquid hold-up measurements.

IV RESULTS AND DISCUSSIONS

4.1 Bubble behaviors in sub-regime air-water slug flow

Figure 2 shows the qualitative visualization of the bubbly tail of sub-regime air-water slug flow for quantifying their behaviors. Bubble behaviors in the bubbly tail, based on the qualitative visualization, defined the sub-regime flow patterns as Initially dispersed Bubbles (IdB), Low dispersed Bubbles (LdB), High dispersed Bubbles (HdB), and Dominantly dispersed Bubbles (DdB). At the bubble tail of IdB, an elongated narrow, shaped bubble that flowed along the upper side of the pipe occurred due to the higher momentum of the liquid, which increased the speed of the flowing bubble, streamlining the bubble nose. High friction along the pipe surface, near thewall, the air-water two-phase flow sheered away from the edge of the pipe. This triggers a transition from the plug into a slug, leading to the bubbles' initial break-up, as shown in **Fig. 2 (a)**. The bubble tail exerted by the high momentum of liquid caused the dispersal of the small bubbles in the liquid slug. Moreover, several bubbles traveled occurred in the slug- bubbly tail.

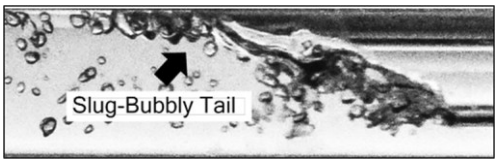

Figure 2a. Bubble behaviors characteristics in sub-regime of air-water slug flow. Initially dispersed Bubbles (IbB) $J_G = 0.70\ \mathrm{m/s}$ and $J_L = 0.44\ \mathrm{m/s}$

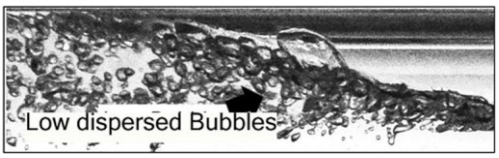

Figure 2b. Bubble behaviors characteristics in sub-regime of air-water slug flow. Low dispersed Bubbles (LdB) $J_G = 1.26\ \mathrm{m/s}$ and $J_L = 0.31\ \mathrm{m/s}$

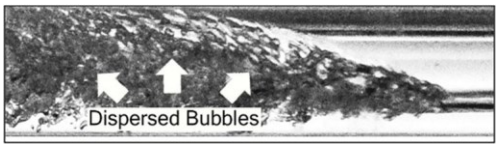

Figure 2c. Bubble behaviors characteristics in sub-regime of air-water slug flow. High dispersed Bubbles (HdB) $J_G = 1.88\ \mathrm{m/s}$ and $J_L = 0.44\ \mathrm{m/s}$

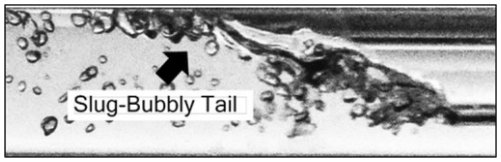

Figure 2d. Bubble behaviors characteristics in sub-regime of air-water slug flow. Dominantly dispersed Bubbles (DdB) $J_G = 6.00\ \mathrm{m/s}$ and $J_L = 0.31\ \mathrm{m/s}$

In the higher momentum of gas, the LdB is a low slug flow of bubbles in the slug-bubbly tail. The LdB flow occurred, as shown in **Fig. 2 (b)**, due to the momentumof the elongated bubble that drives the slug liquid phase to flow at a faster velocity. The elongated bubble momentum affects the development of the slug [21]. The superficial velocity of the gas is higher than the IdB; hence, the slug-bubbly tail is moreaerated. The higher momentum of both gas and liquid shows the linear tendency. As shown in **Fig. 2 (c)**, the HdB is the numerous dispersed bubbles in the slug-bubbly tail. They are also known as aeration. They occur continuously and intensively at the air-water interface, inside the slug-bubbly tail [22], where the liquid slug is more aerated and becomes chaotic than within LdB. The higher momentum of the gas.

Affects the entrainment in the liquid slug front traveled to the slug-bubbly tail. The traveled bubbles in HdB penetrated the interface of the slug tail and disrupted the elongated thin layer of bubbles. The DdB is defined as the HdB with a wavy interface. **Fig.2 (d)** shows how the wavier interface at the liquid slug front and slug-bubbly tail are more chaotic than HdB. The smaller dispersed bubbles disrupted the elongated bubbles and caused the wavy interfaces. The dynamic changes of gas and liquid momentum led to different characteristics of sub-regimes of air-water slug flow based on the four proposed flows. The massive dispersed bubbles in the highest momentum caused structural damage to the elbow, knee, tee, nozzle, and diffuser.

Figure 3 shows the quantified bubble behaviors obtained from Eq. (5) in sub-regimes of air-water slug flow. The quantification of the four characteristics of sub-regime air-water slug flow in the horizontal pipe was based on the bubble behaviors obtained by qualitative visualization. Gas and high liquid momentum forced the bubbles to be distributed in the wider area inside the slug-bubbly tail.

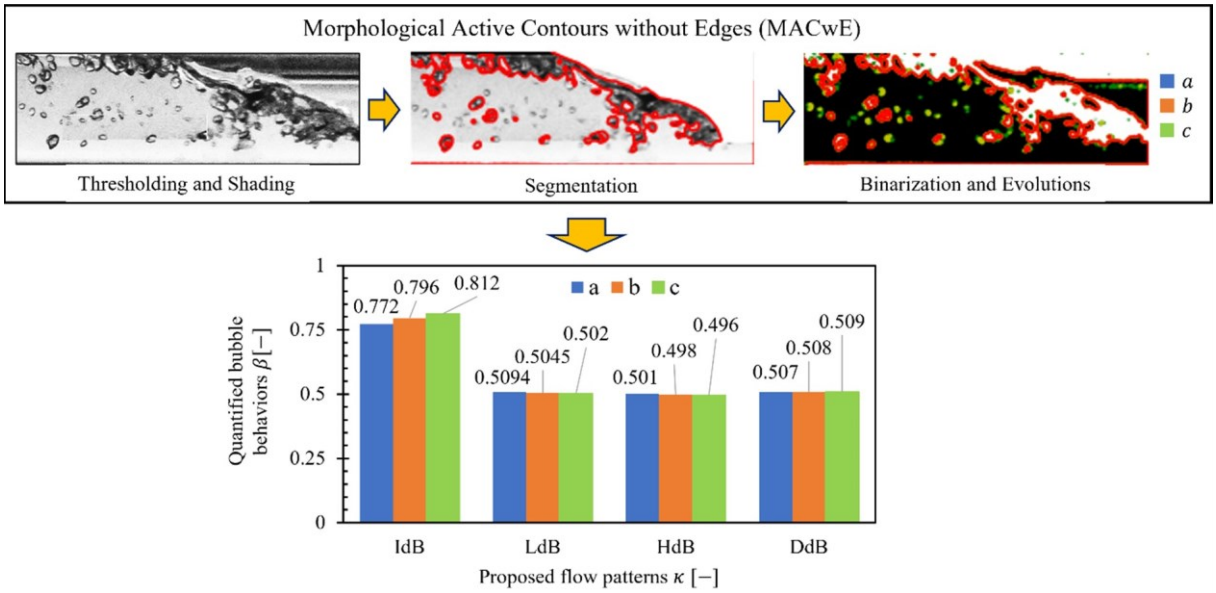

Figure 3. Quantified bubble behaviors β in the sub-regime of air-water slug flow.

4.1 Characteristics of sub-regime air-water slug flow by LHmBb

Figure 4 shows the liquid hold-up obtained from Eq. (6) in sub-regimes of air-water slug flow. The characteristics of sub-regime air-water slug flow are divided into three stages which are 1) the occurrence of liquid plug reflected by the probability density function P at the liquid hold-up α = 0.8 —[—], 2) the occurrence of plug bubbles represented the dispersed bubble behaviors reflected by P at α = 0.4 — 0.8 [—], and 3) the high momentum of slug bubbles symbolized the higher momentum of dispersed bubble behaviors reflected by P at α = 0.1 — 0.3 [—]. The initially dispersed bubble (IdB) flow has a higher momentum than slug bubbles, as shown in **Fig. 4 (a)**. Four different segmentations in heights denoted as y were proposed with a distance of $0.25D$ to illustrate characterization as seen from the distribution of brightness level B to the observed length x, the bubbles dispersed were observed by the low fluctuation of B alongside x. The linear tendency of the increasing number of dispersed bubbles and the momentum was correlated to the increasing P at lower α. From the mass conservations view, the smaller size of dispersed bubbles distributes uniformly, leading to lower momentum compared with the liquid plug under IdB. These are validated by the changes of distribution of P from α = 0.8 — 1.0 [—] under LdB and HdB to α = 0.1 — 0.3 [—] under DdB. Moreover, the frequency of B alongside x is dense, agreeing with the tendency of static pressure and slug frequency proposed by [2]and [3]. The approach based on image processing was infeasible for industrial applications. The *in situ* measurements based on LH correlated to the bubble behaviors are good for the rapid decision making on the real scale ofair-water two-phase flow.

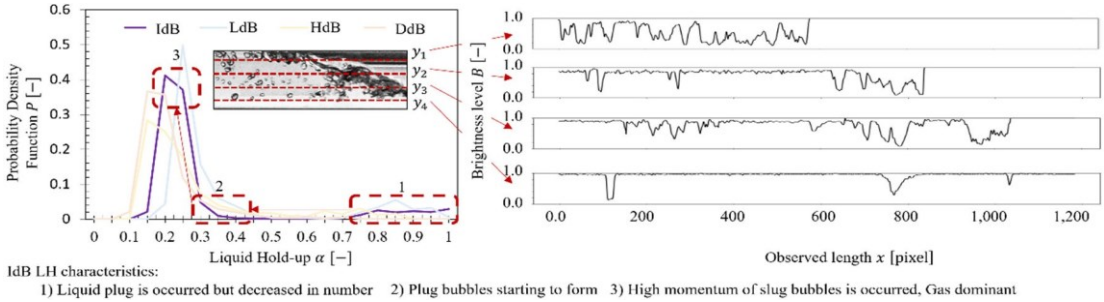

Figure 4a. Liquid hold-up α characteristics in sub-regime of air-water slug flow. Initially dispersed Bubbles (IbB) $J_G = 0.70\ \mathrm{m/s}$ and $J_L = 0.44\ \mathrm{m/s}$

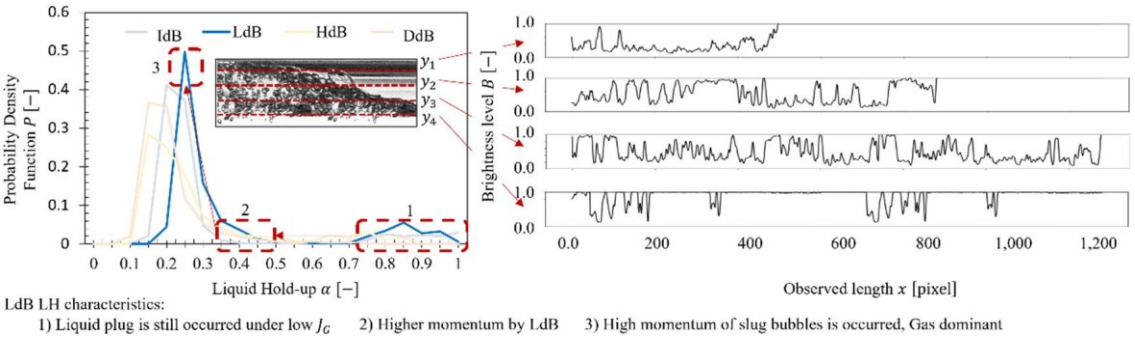

Figure 4b. Liquid hold-up α characteristics in sub-regime of air-water slug flow. Low dispersed Bubbles (LdB) JG = 1.26 m/s and JL = 0.31 m/s

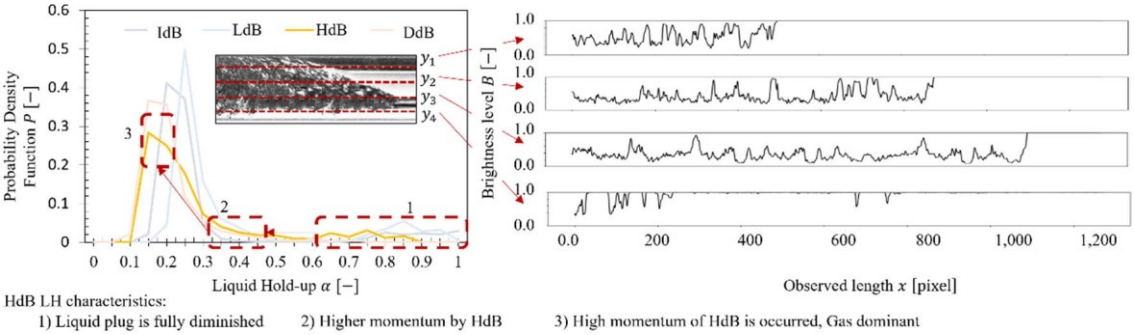

Figure 4c. Liquid hold-up α characteristics in sub-regime of air-water slug flow High dispersed Bubbles (HdB) JG = 1.88 m/s and JL = 0.44 m/s

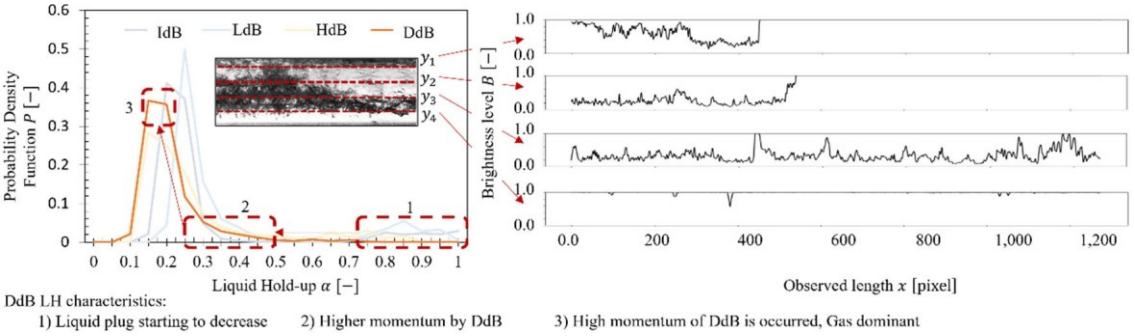

Figure 4d. Liquid hold-up α characteristics in sub-regime of air-water slug flow. Dominantly dispersed Bubbles (DdB) JG = 6.00 m/s and JL = 0.31 m/s

4.2 Correlation function of LHmBb for predicting sub-regime air-water slug flow

Figure 5 shows the correlation function of LHmBb for predicting sub-regime air-water slug flow in horizontal pipe based on three dominant liquid hold-ups α defined in **section 4.2**. Each α is defined as the average value within the three stages. The most dominant value of probability density function P is plotted in three α based on the three points for the simplified polynomial correlation function as,

$$P' = \varsigma_1\alpha^2 - \varsigma_2\alpha + \varsigma_3 \qquad (8)$$

Equation (7) is solved in **Table 1**. As shown in **Fig. 5**, the three stages were used to predict sub-regime air-water slug flow characteristics with the pivot α, which determines the changes in flowpatterns. Moreover, the correlation function of LHmBB P' has a low error based on the comparison between P and P. 'To provide comprehensive validations, the proposed P' was planned to be verified by previous models and tested as the input of a machine learning application for predicting the α, flow regimes, and bubble velocities.

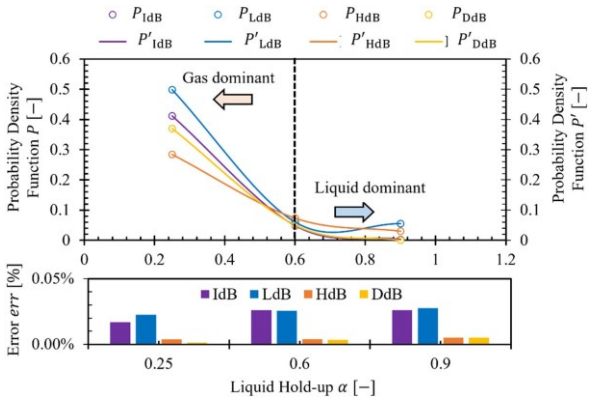

Figure 5. Liquid hold-up characteristics in sub-regime of air-water slug flow.

Table 1 Coefficients and error rate of the proposed correlation function P'.

κ	ς_1[—]	ς_2[—]	ς_3[—]	$\langle err \rangle$[%]
IdB	1.366	2.200	0.876	0.023
LdB	1.899	2.866	1.096	0.025
HdB	0.707	1.204	0.541	0.004
DdB	1.150	1.892	0.771	0.003

V CONCLUSION

In this study, the characteristics of the sub-regimes of air-water slug flow in the horizontal pipe by the proposed liquid hold-up model correlated to bubble behaviors (LHmBb) can be summarized as follows.

The quantified bubble behaviors in terms of β were obtained by the image processing technique based on the active morphological contour without edge (MACwE) technique processed in Python 3.8. The β is decreasing under different flow regimes and gives a minor explanation of the bubble distribution in the sub-regimes air-water slug flow. The difference of β is caused by the less sensitivity of β_H obtained from MACwE. An improved algorithm provided a more detailed segmentation, and binarization was planned for the future works,

The LHmBb successfully determined the sub-regimes air-water slug flow characteristics with qualitative analysis and provide the understanding of the previous works. The four characteristics, defined as Initially dispersed Bubbles (IdB), Low dispersed Bubbles (LdB), High dispersed Bubbles (HdB), and Dominantly dispersed Bubbles (DdB), provided a new finding regarding the sub-regimes air-water slug flow in a horizontal pipe.

The correlation function offered a high accuracy prediction of the air-water slug flow regimes sub-regimes. A comprehensive correlation was required to elaborate on the important slug flow mechanism and contribute to the development of air-water two-phase flow in a multiphase flow society.

Acknowledgments

This research as accomplished within a research project funded by the Directorate General of Higher Education, Ministry of Education and Culture, Republic of Indonesia. The project number is LPPM-UGM/1448/LIT/2013. The authors express gratitude to the technical support from Mr. A. Widyatama, Mr. T.F. Sinaga, Mr. R.R. Muhamad, and Mrs. R.S. Sarworo.

References

[1] J. Villarreal, D. Laverde, and C. Fuentes, "Carbon-steel corrosion in multiphase slug flow and CO2," *Corros. Sci.*, vol. 48, no. 9, pp. 2363–2379, 2006,

doi: 10.1016/j.corsci.2005.09.003.

[2] O. Dinaryanto *et al.*, "Experimental investigation on the initiation and flow development of gas-liquid slug two-phase flow in a horizontal pipe," *Exp. Therm. Fluid Sci.*, vol. 81, pp. 93–108, Feb. 2017.

[3] A. Arabi, Y. Salhi, Y. Zenati, E. K. Si-Ahmed, and J. Legrand, "On gas-liquid intermittent flow in a horizontal pipe: Influence of sub-regime on slug frequency," *Chem. Eng. Sci.*, vol. 211, p. 115251, 2020, doi: 10.1016/j.ces.2019.115251.

[4] M. Fernandino and T. Ytrehus, "Determination of flow sub-regimes in stratified air-water channel flow using LDV spectra," *Int. J. Multiph. Flow*, vol. 32, no. 4, pp. 436–446, 2006, doi: 10.1016/j.ijmultiphaseflow.2006.01.003.

[5] Y. Taitel and A. E. Dukler, "A model for predicting flow regime transitions in horizontal and near horizontal gas-liquid flow," *AIChE J.*, vol. 22, no. 1, pp. 47–55, 1976, doi:10.1002/aic.690220105.

[6] P. Y. Lin and T. J. Hanratty, "Prediction of the initiation of slugs with linear stability theory,"

Int. J. Multiph. Flow, vol. 12, no. 1, pp. 79–98, 1986, doi: 10.1016/0301-9322(86)90005-4.

[7] E. T. Hurlburt and T. J. Hanratty, "Prediction of the transition from stratified to slug and plug flow for long pipes," *Int. J. Multiph. Flow*, vol. 28, no. 5, pp. 707–729, 2002, doi: 10.1016/S0301-9322(02)00009-5.

[8] P. Andreussi, A. Di Donfrancesco, and M. Messia, "An impedance method for the measurementof liquid hold-up in two-phase flow," *Int. J. Multiph. Flow*, vol. 14, no. 6, pp. 777–785, 1988, doi: 10.1016/0301-9322(88)90074-2.

[9] T. Fukano, "Measurement of time varying thickness of liquid film flowing with high-speed gas flow by a constant electric current method (CECM)," *Nucl. Eng. Des.*, vol. 184, no. 2–3, pp. 363–377, 1998, doi: 10.1016/S0029-5493(98)00209-X.

[10] O. Dinaryanto, A. Widyatama, M. Prestinawati, Indarto, and Deendarlianto, "The characteristics of the sub regime of slug flow in 16 mm horizontal pipe," *AIP Conf. Proc.*, vol. 2001, 2018, doi: 10.1063/1.5049980.

[11] A. Setyawan, Indarto, and Deendarlianto, "Simplified correlation for liquid hold-up in a horizontal two-phase gas-liquid annular flow," *J. Adv. Res. Fluid Mech. Therm. Sci.*, vol. 62, no.1, pp. 20–30, 2019.

[12] Deendarlianto, T. Höhne, P. Apanasevich, D. Lucas, C. Vallée, and M. Beyer, "Application of a new drag coefficient model at CFD-simulations on free surface flows relevant for the nuclear reactor safety analysis," *Ann. Nucl. Energy*, vol. 39, no. 1, pp. 70–82, 2012, doi: 10.1016/j.anucene.2011.09.010.

[13] A. W. O. D. K. I. Deendarlianto Moeso Andrianto, "CFD Studies on the gas-liquid plug two- phase flow in a horizontal pipe," *J. Pet. Sci. Eng.*, vol. 147, pp. 779–787, Sep. 2016, doi: 10.1016/j.petrol.2016.09.019.

[14] K. Tanaka, Y. A. K. Prayitno, P. A. Sejati, D. Kawashima, and M. Takei, "Void Fraction Estimation in Vertical Gas-Liquid Flow by Plural Long Short-term Memory with Sparse Model Implemented in Multiple Current-Voltage System (pLSTM-SM-MCV)," *Multiph. Sci. Technol.*, 2021, doi: 10.1615/multscientechn.2021039801.

[15] Y. A. K. Prayitno, T. Zhao, Y. Iso, and M. Takei, "In situ measurement of sludge thickness in high-centrifugal force by optimized particle resistance normalization for wireless electrical resistance detector (WERD)," *Meas. Sci. Technol.*, vol. 32, no. 3, p. 034001, Mar. 2021, doi:10.1088/1361-6501/abc108.

[16] A. Widyatama, O. Dinaryanto, Indarto, and Deendarlianto, "The development of image processing technique to study the interfacial behavior of air-water slug two-phase flow in horizontal pipes," *Flow Meas. Instrum.*, vol. 59, no. October 2017, pp. 168–180, 2018, doi: 10.1016/j.flowmeasinst.2017.12.015.

[17] W. E. Juwana, A. Widyatama, O. Dinaryanto, W. Budhijanto, Indarto, and Deendarlianto, "Hydrodynamic characteristics of the microbubble dissolution in liquid using orifice type microbubble generator," *Chem. Eng. Res. Des.*, vol. 141, pp. 436–448, 2019, doi: 10.1016/j.cherd.2018.11.017.

[18] Deendarlianto, A. Z. Hudaya, Indarto, and K. D. Ozzilenda Soegiharto, "Wetted wall fraction of gas-liquid stratified co-current two-phase flow in a horizontal pipe with low liquid loading," *J. Nat. Gas Sci. Eng.*, vol. 70, no. May, p. 102967, 2019, doi: 10.1016/j.jngse.2019.102967.

[19] P. M. Ujang, C. J. Lawrence, C. P. Hale, and G. F. Hewitt, "Slug initiation and evolution in two-phase horizontal flow," *Int. J. Multiph. Flow*, vol. 32, no. 5, pp. 527–552, 2006, doi: 10.1016/j.ijmultiphaseflow.2005.11.005.

[20] A. Kawahara, P. Y. Chung, and M. Kawaji, "Investigation of two-phase flow pattern, void fraction and pressure drop in a microchannel,"

Int. J. Multiph. Flow, vol. 28, no. 9, pp. 1411–1435, 2002, doi: 10.1016/S0301-9322(02)00037-X.

[21] J. Thaker and J. Banerjee, "Characterization of two-phase slug flow sub-regimes using flow visualization," *J. Pet. Sci. Eng.*, vol. 135, pp. 561–576, 2015, doi: 10.1016/j.petrol.2015.10.018.

[22] A. Arabi, Y. Salhi, A. Bouderbal, Y. Zenati, E. K. Si-Ahmed, and J. Legrand, "Onset of intermittent flow: Visualization of flow structures," *Oil Gas Sci. Technol.*, vol. 76, no. April, 2021, doi: 10.2516/ogst/2021009.

FREE 1 (2022) 23-30

Frontiers in Renewable Energy (FREE)

Journal homepage: www. https://jurnal.ugm.ac.id/v3/FREE/

Application of Analytic Hierarchy Process in the Selection of *Botryococcus braunii* Cultivation Technology for Bio-crude Oil Production

Ferliandi[1], Eko Agus Suyono[2], Nugroho Dewayanto[1,3], and Arief Budiman[3]

[1] Master Program in System Engineering, Universitas Gadjah Mada
Jalan Teknika Utara 3, Barek, Yogyakarta 55281, Indonesia
[2] Faculty of Biology, Universitas Gadjah Mada
Jalan Teknika Selatan, Yogyakarta 55281, Indonesia
[3] Center of Excellence for Microalgae Biorefinery, Center for Energy Studies, Universitas Gadjah Mada
Sekip K1A, Kampus UGM, Yogyakarta 55281, Indonesia

ARTICLE INFO

Article history:
Received 19 January 2022
Revised 14 February 2022
Accepted 8 April 2022
Available online 10 August 2022

Key words:
Botryococcus braunii, Cultivation System, Analytic Hierarchy Process

ABSTRACT

Bio-crude oil is obtained through a thermochemical process of biomass and can be used to reduce the Indonesian government's dependence on fossil energy. A potential source of biomass that is generally used for bioenergy production is microalgae, with *Botryococcus braunii* as the promising type. In the conversion of microalgae into bio-crude, the cultivation section is among the units required. Therefore, this study aims to determine the most effective and optimal cultivation technology that can be applied to the bio-crude oil refinery plant. It was carried out at the cultivation simulation system in Cilacap, Central Java, Indonesia, using the Analytic Hierarchy Process (AHP) method. The criteria used were the reactor land area requirement, energy consumption, water usage, cost, contamination risk, ease of scale-up, and adaptation ability to weather changes. Meanwhile, the proposed alternative systems were open raceway pond, flat-panel photo-bioreactor, hybrid, and membrane photo-bioreactor. The AHP results showed that the open raceway pond was selected for application in the bio-crude oil refinery process. The biomass production potential of *B. braunii* from the cultivation unit was 19.8795 ton/year/ha, which can be processed into 11.5301 ton of bio-crude oil with a high heating value (HHV) of 553,448.8 MJ.

I. INTRODUCTION

The derivation of Indonesia's primary energy mix from new and renewable energy (NRE) is still very low. Based on the latest data before the Covid-19 pandemic, only 9.18% of the total national primary energy supply of 1,620.69 million Barrel of Oil Equivalent (BOE) was provided by NRE [1] while others are dominated by oil, natural gas, and coal. Meanwhile, biofuel is a form of using NRE, which supplied approximately 2.95% of primary energy in 2019.

Bio-crude oil is the application of biofuel as alternative energy and is a blackish compound containing various

Peer review under responsibility of Frontiers in Renewable Energy (FREE).
*Corresponding author.
E-mail address: abudiman@ugm.ac.id (Arief Budiman)

hydrocarbons similar to petroleum-based on its straight-chain hydrocarbon content [2]. In its production, processes such as cleaning, hydrotreating, and hydrocracking are required to remove oxygen and heavy compounds to produce a drop in biofuel [3, 4]. Bio-crude oil can be obtained through thermochemical processes on biomass such as fast pyrolysis and hydrothermal liquefaction (HTL) [5]. The main difference between these technologies is the use of dry feedstock in fast pyrolysis, while wet stock is applied in HTL [6]. Furthermore, the oil from HTL has an oxygen content of 10-20 wt.%, which is much lower than 40 wt.% in pyrolysis. This property is due to the calorific value of HTL that is higher than pyrolysis with, 35 MJ/kg and 16-19 MJ/kg, respectively and is comparable to the 40-45 MJ/kg of conventional petroleum fuel [7].

Microalgae is a promising source of biomass that can be processed into bio-crude oil. It is derived from non-food raw materials and can be cultivated on relatively small lands. Furthermore, it has high photosynthetic efficiency, growth rate, biomass productivity, and good capacity to use water, CO_2, and sunlight to synthesize biomass via photosynthesis [8]. In this study, the microalgae species used was *Botryococcus braunii* which is a green colony freshwater microalga that produces hydrocarbons [9] and can be found in all climatic zones except Antarctica [10]. Although *B. braunii* is a type of freshwater microalgae, it has been investigated in cultivation using sea/brackish water media [11; 12]. Meanwhile, the use of seawater is more desirable in industrial-scale culture due to the reduction of the risk of contamination by other freshwater-living organisms in culture ponds [12]. *B. braunii* has a wide temperature tolerance range from -20 to 40^{o}C, which makes the large-scale outdoor cultivation to be carried out because of the minimal effect of extreme temperature shifts on the growth rate [13; 14]. The content of carbon and hydrogen, as well as the high heating value (HHV) which is within 32.9–54.7 MJ/kg in the biomass of this algae has a higher value than other types of microalgae [15]. *B. braunii* has also been considered a slow-growing alga with a generation time of 7 days in nature [16], while the Showa strain shows that it has a fast growth rate of 1.4 days [17]. Recently, it was discovered that there are 9 fast-growing strains with faster growth rates or similar to the Showa strain [18]. A previous report also stated that some of the properties of *B. braunii* crude oil are comparable to diesel oil, except for its higher kinematic viscosity [19]. Therefore, this study aims to select the optimal cultivation system for processing biomass from the *B. braunii* into bio-crude oil.

The selection of proper cultivation technology for *B. braunii* becomes a crucial decision since it will affect the whole aspect of the production of bio-crude oil. Meanwhile, the preferred technology needs to provide the best quality of biomass as indicated by yield and growth rate, the complexity of the process, energy consumption, operating cost, and economical aspects. Previous reports have shown that the Analytical Hierarchy Process (AHP) can be applied to make decide on the selection of several alternatives. In this study, AHP was used to compare and decide the best cultivation technology for *B. braunii*.

II. METHODOLOGY

The Analytical Hierarchy Process (AHP) method was used to analyze several criteria in selecting the preferred cultivation system.

2.1 Structure of Analytical Hierarchy Process (AHP)

AHP is a hierarchical structure-based tool developed by Thomas L. Saaty to manage qualitative and quantitative multi-criteria elements involved in decision-making behavior [19]. The basic concept of AHP is the use of pairwise comparison matrices [20], where the pair comparison scales are called the intensity of importance scale (table 1). Subsequently, the priority vector (weight) was calculated from that the pairwise comparison matrices using the eigenvector method. This method is popularly used to method to estimate a priority vector as proposed by Saaty [21].

Table 1. Intensity of importance scale [18]

Intensity of importance	Definition	Explanation
1	Equal importance	Two activities contribute equally to the objective
3	Moderate importance of one over another	Experience and judgment strongly favor one activity over another
5	Essential or strong importance	Experience and judgment strongly favor one activity over another

7	Very strong importance	Activity is strongly favored and its dominance demonstrated in practice
9	Extreme importance	The evidence favoring one activity over another is of the highest possible order of affirmation
2,4,6,8	Intermediate values between the two adjacent judgments	When compromise is needed
Reciprocals	When activity i has one of the above numbers assigned to it when compared with activity j, then j has the reciprocal value	

The hierarchical structure was divided into 3 levels (figure 1). Moreover, level 1 was the study goal, which was to select a cultivation system for bio-crude oil production. Level 2 was the qualitative and quantitative criteria used for the selection. The land area of the reactor, energy consumption, water usage, and cost were the quantitative criteria, while contamination risk, ease of scale-up, and adaptation ability to weather changes were the qualitative criteria. Level 3 was the alternative of cultivation systems, which include open raceway pond (ORP), flat panel photo-bioreactor (FP-PBR), hybrid, and membrane photo-bioreactor (MPBR).

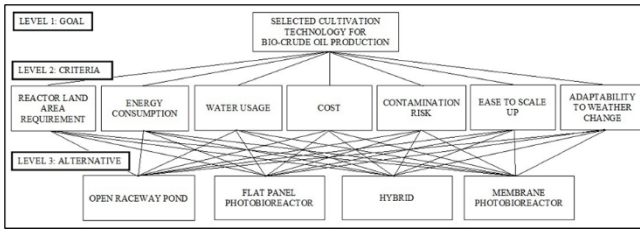

Figure 1. Analytical hierarchy process structure of this case study

2.2 Cultivation System Simulation Site Characteristics

The secondary data used in this study were derived from government reports and the results of previous studies. Subsequently, the location for the cultivation system simulation was in Cilacap Regency. It was selected due to its closeness to abundant water sources from the sea, the existence of oil refineries unit nearby for co-processing between bio-crude oil and crude oil, free carbon source (CO_2), and a dock for the delivery of processing products via sea transportation. The area of land available for the construction of the cultivation system including the utility area is 8 ha. Based on Figure 2, the cultivation simulation had an annual average global horizontal solar radiation of 1,915 kWh/m^2 or 5.25 kWh/m^2/day, while the annual average temperature from 2015 to 2020 of the location was 27.2°C [22].

Figure 2. Characteristics of the cultivation system simulation site

The biomass productivity of *B. braunii* cultivated in ORP from previous reports with similar characteristics was 0.114 g/L/day [23], which was conducted at an ambient temperature of 29°C, solar radiation of 5 kWh/m^2/day, and air humidity of 71% at a harvesting time of 15 days. During cultivation, a total of 200 L seed culture of *B. braunii* was grown in mini ORP with a biomass concentration of 0.085 g/L. Subsequently, it was transferred to the 2000 L ORP containing 1800 L of modified CHU 13 medium.

The productivity of *B. braunii* cultivated in FP-PBR used reference with a value of 292.5 mg/L/day of biomass [24]. This was carried out using 30 L PBR filled with BG-11 nutrient medium, operating at 0.33 vvm air flow rate & 1% CO_2. The productivity values were calculated on the 4th day of cultivation under the temperature of 27°C, a light intensity of 1,000 µmol/m^2/s, and a maximum biomass concentration of 1.17 g/L. Since 2.02 µmol/m^2/sec photon photosynthetically active radiation (PAR) is equivalent to 1 W/m^2 solar radiation [25], therefore, 1,000 µmol/m^2/s is equal to 5.45 kWh/m^2/day (11 hours of daylight).

In a hybrid cultivation system, productivity was the combination of these two values. Meanwhile, the MPBR productivity has been calculated as 2 times greater than the optimum productivity of PBR, namely for the submerged biomass retention MPBR [26].

The yield of bio-crude oil from the HTL process on the microalgae biomass of *B. braunii* from previous results varied from 4.04 wt% [2] to 58 wt% [27, 28] and 68 wt% [29]. This study used a yield value of 58 wt% to calculate the produced bio-crude oil, however, it was reported that the high heating value in the bio-crude oil was 48 MJ/k [27, 28].

III RESULTS AND DISCUSSION

In this study, the data processing to obtain the value of the intensity of importance scale was completed through 2 methods. In the first approach, the procedure was carried out by calculating the system design based on previous reports. Subsequently, the pairwise comparisons between systems were carried out using the results of these calculations to get the intensity of importance scale to assess the quantitative criteria for alternatives at level 3. In the second method, pairwise comparisons were assessed by respondents (experts) through questionnaires. This was applied to the comparison between criteria at level 2 and the assessment of qualitative criteria against alternatives at level 3.

3.1 Criteria Weight Calculation (Level 2)

The pairwise comparison scale at level 2 was formed from the average assessment made by expert respondents on the contribution of each element (criteria) to achieve the goal. This was carried out to determine the order of importance of the 7 criteria used according to the experts based on the characteristics of the location. From Figure 3, the weighting result showed that the investment cost is the most influential criterion, followed by energy consumption, reactor land area requirement, ease to scale up, water usage, contamination risk, and adaptability to weather change.

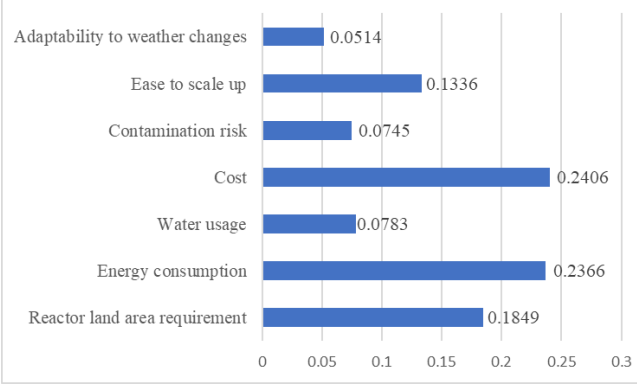

Figure 3. Chart of the weight of each criterion

3.2 Calculation of Alternative Local Weights Against Criteria (Level 3)

The definition of the criteria for the reactor land area requirement was the area required for the cultivation system to produce the same product as the open raceway pond which was built on 8 ha. Meanwhile, the 4 cultivation systems were assumed to have the same utility area and the open raceway pond design is shown in figure 4 [30]. The assumption of effective production time per year was 330 days as used in previous studies [31; 32]. It was discovered that a total of 8 units of open raceway ponds including the utility area can be built in those available land areas with a projected biomass production yield of 79.5179 tons/year.

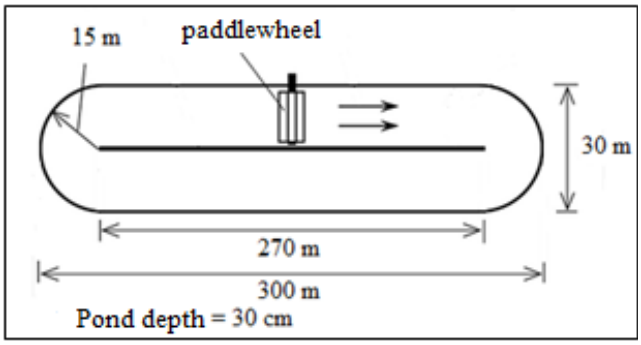

Figure 4. The open raceway pond design

The FPBR design is shown in figure 5 [30; 33], while the land area to build flat panel PBR which was needed for the same production projection as the open raceway pond was 2.4033 ha.

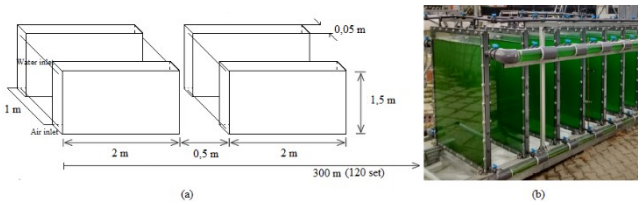

Figure 5. The flat panel PBR design

The hybrid cultivation system was designed by combining 1 unit of ORP and FP-PBR. This system required an area of 3.0950 ha to produce the same amount of biomass, while the MPBR used the design basis of the FP-PBR. The use of reactors with a short light path like the flat panel to construct MPBR is generally recommended [34] and the land area required to build that MPBR was 1.6788 ha.

The energy consumption was the one required for the cultivation system to operate by volume within 330 days per year. The water usage criterion was the flow

rate per day needed by the system to maintain the dilution rate. Meanwhile, the cost criterion was the production cost for total biomass of 79.5179 tons within 1 year. The results of the three quantitative criteria are shown in Tables 2-4.

Table 2. Energy consumption of each alternative

No	Alternative	Power or Energy Consumption per Reactor Volume	Volume (m^3)	Energy per 1 Year of Production (MW)
1.	ORP	4 W/m^3 [35]	2113.712	66.9624
2.	FP-PBR	53 W/m^3 [36]	828	347.5613
3.	Hybrid	Combination of ORP & PBR	984.214	310.5975
4.	MPBR	0.64 kWh/m^3 [37]	414	2098.4832

Table 3. Flow rate of each alternative

No	Alternative	Reactor Volume (m^3)	Flow rate ($F=D\times V$; m^3/day)
1.	ORP	2113.7120	528.4280
2.	FP-PBR	828	207
3.	Hybrid	245.5535	245.5535
4.	MPBR	414	103.5

Table 4. Cost of biomass production of each alternative

No	Alternative	Production cost per Kg	Total Production Cost per Year
1.	ORP	€ 4.95 [38]	€ 393,613.61
2.	FP-PBR	€ 5.96 [38]	€ 473,926.68
3.	Hybrid	Combination of ORP & PBR	€ 463,887.73
4.	MPBR	US$11.30 [39]	€ 790,726.00

Note: US $1 = € 0.88

The contamination risk criteria were the risk level of a cultivation system that can be disturbed by an external predator. The ease to scale up criterion was assessed for each system based on its technology maturity and commercial company availability for its development from the laboratory to large scale. Meanwhile, the adaptability to weather change criterion was the ability of a cultivation system to continue production without being affected by weather changes. The pairwise comparison from the assessment result of the three qualitative criteria is shown in Table 5.

The weighting results of alternatives against criteria are summarized in Table 6 and are in line with previous studies for most of the criteria that compared ORP, PBR, and hybrid [40] and discussed membrane application in PBR, namely MPBR [41]. The higher the weight value of a cultivation system, the more preferred the system in terms of related criteria. This is indicated by the reactor land area requirement, which was wider on ORP than the others, making its weight value the lowest. Since MPBR energy consumption was the highest, it had the lowest weight value.

On the contamination risk criterion, FP-PBR had a higher weight than MPBR, although both systems had the same design basis. This result showed that based on previous reports and existing applications, respondents preferred FP-PBR to MPBR to face the risk of contamination. Meanwhile on the cost criteria, the difference between the ORP and FP-PBR was not significant, hence it has the same weight in the AHP calculation.

Table 5. Pairwise comparison for qualitative criteria

Pairwise comparison	ORP	FP-PBR	Hybrid	MPBR
Contamination risk				
ORP	1	1/5	1/4	1/5
FP-PBR	5	1	3	3
Hybrid	4	1/3	1	1
MPBR	5	1/3	1	1
Ease to scale up				
ORP	1	5	4	5
FP-PBR	1/5	1	1	4
Hybrid	1/4	1	1	3
MPBR	1/5	1/4	1/3	1
Adaptability to weather change				
ORP	1	1/4	1/3	1/4
FP-PBR	4	1	3	2
Hybrid	3	1/3	1	1/4
MPBR	4	1/2	4	1

Table 6. Weighting results of Level 3

Criteria	ORP	FP-PBR	Hybrid	MPBR
Reactor land area requirement	0.0819	0.2346	0.2107	0.4394
Energy consumption	0.6271	0.1631	0.1720	0.0378
Water usage	0.0922	0.2384	0.2155	0.4539
Cost	0.2857	0.2857	0.2857	0.0632
Contamination risk	0.0632	0.5101	0.2057	0.2210
Ease to scale up	0.5908	0.1751	0.1658	0.0683
Adaptability to weather changes	0.0757	0.4403	0.1430	0.3410

I. Global Weight Calculation

The global weight was calculated to determine the final goal, which was the selection of a cultivation system for bio-crude oil production. This was carried out for the four alternatives by multiplying each local weight against the related criteria and the results were summed as shown in Figure 6.

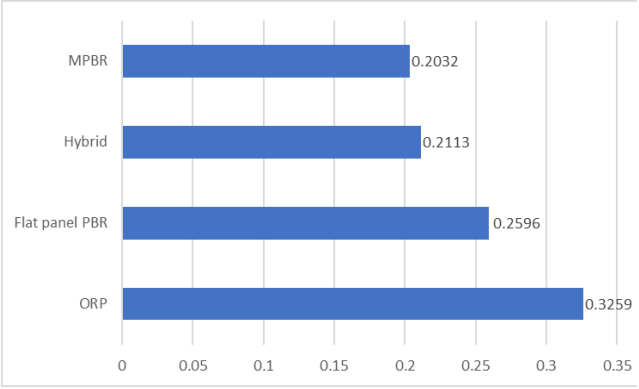

Figure 6. Global weight of each alternative

Based on the global weight calculation, the ORP had the highest weight value, followed by flat-panel PBR, hybrid, and MPBR.

IV. CONCLUSION

Several technologies are available for the cultivation of *B. braunii* for bio-crude oil production. Based on the AHP method, the best alternative cultivation system was the open raceway pond, followed by PBR flat panel, hybrid, and MPBR with the yields of 0.3259, 0.2596, 0.2113 and 0.2032, consecutively.

The biomass production potential was 79.5179 ton/year for an open raceway pond with a land area of 8 ha or 19.8795 tons/year/ha. According to the HTL yield value of 58 wt%, the bio-crude oil that can be produced from the cultivation system was 11.5301 tons/year with an HHV of 553,448.8 MJ/year.

References

[1] Ministry of Energy and Mineral Resources Republic of Indonesia, Handbook of Energy and Economic Statistics of Indonesia 2019, Jakarta: Center for Data and Information Technology on Energy Mineral Resources, 2020.

[2] L. Prasakti, R. Rochmadi, and A. Budiman, "The Effect of Biomass-Water Ratio on Bio-crude Oil Production from Botryococcus braunii using Hydrothermal Liquefaction Process," Jurnal Rekayasa Proses, vol. 13, no.2, pp.132-138, 2019.

[3] H. K. S. Panahi, M. Tabatabaei, M. Aghbashlo, M. Dehhaghi, M. Rehan, and A. S. Nizami, "Recent updates on the production and upgrading of bio-crude oil from microalgae," Bioresource Technology Reports, vol. 7, no. 100216, 2019.

[4] Y. Zhu, M. J. Biddy, S. B. Jones, D. C. Elliott, and A. J. Schmidt, "Techno-economic analysis of liquid fuel production from woody biomass via hydrothermal liquefaction (HTL) and upgrading," Applied Energy, vol. 129, pp.384–394, 2014.

[5] U.S. Department of Energy, Waste-to-Energy from Municipal Solid Wastes, Washington, DC: Office of Energy Efficiency and Renewable Energy, 2019.

[6] Y. Zhu, M. J. Biddy, S. B. Jones, D. C. Elliott, and A. J. Schmidt, "Techno-economic analysis of liquid fuel production from woody biomass via hydrothermal liquefaction (HTL) and upgrading," Applied Energy, vol. 129, pp.384–394, 2014.

[7] A. Demirbas, "Competitive liquid biofuels from biomass," Applied Energy, vol. 88, no. 1, pp.17–28, 2011.

[8] Z. Yin, L. Zhu, S. Li, T. Hu, R. Chu, F. Mo, D. Hu, C. Liu, and B. Li, "A comprehensive review on cultivation and harvesting of microalgae for biodiesel production: Environmental pollution control and future directions," Bioresource Technology, vol. 301, Jan., no. 122804, 2020.

[9] A. R. Rao, G. A. Ravishankar, and R. Sarada, "Cultivation of green alga *Botryococcus braunii* in raceway , circular

ponds under outdoor conditions and its growth, hydrocarbon production," Bioresource Technology, vol. 123, pp.528–533, 2012.

[10] M. B. Tasic, L. F. R. Pinto, B. C. Klein, V. B. Veljković, and R. M. Filho, "*Botryococcus braunii* for biodiesel production," Renewable and Sustainable Energy Reviews, vol. 64, pp.260–270, 2016.

[11] A. M. Sari, H. E. Mayasari, and S. Zullaikah, "Pertumbuhan dan kandungan lipida dari *Botryococcus braunii* dalam media air laut," Jurnal Teknik Pomits, vol. 2, no. 1, pp.1–6, 2013.

[12] K. Furuhashi, K. Saga, S. Okada, and K. Imou, "Seawater-Cultured *Botryococcus braunii* for efficient hydrocarbon extraction," PLoS ONE, vol. 8, no. 6, pp.1–5., 2013.

[13] M. Demura, M. Ioki, M. Kawachi, N. Nakajima, and M. M. Watanabe, "Desiccation tolerance of *Botryococcus braunii* (*Trebouxiophyceae*, *Chlorophyta*) and extreme temperature tolerance of dehydrated cells," Journal of Applied Phycology, vol. 26, pp.49–53, 2014.

[14] N. S. M. Aron, K. S. Khoo, K.W. Chew, A. Veeramuthu, J. S. Chang, and P. L. Show, "Microalgae cultivation in wastewater and potential processing strategies using solvent and membrane separation technologies," Journal of Water Process Engineering, vol. 39, no. 101701, 2021.

[15] J. Jin, C. Dupré, K. Yoneda, M. M. Watanabe, J. Legrand, and D. Grizeau, "Characteristics of extracellular hydrocarbon-rich microalga *Botryococcus braunii* for biofuels production: Recent advances and opportunities," Process Biochemistry, vol. 51, no. 11, pp.1866–1875, 2016.

[16] J. G. Qin and Y. Li, "Optimization of the growth environment of *Botryococcus braunii* strain CHN 357," Journal of Freshwater Ecology, vol. 21, no. 1, Mar., pp.169-176, 2011.

[17] T. Yoshimura, S. Okada, and M. Honda, "Culture of the hydrocarbon producing microalga *Botryococcus braunii* strain Showa: optimal CO_2, salinity, temperature, and irradiance conditions," Bioresource Technology, vol. 133, pp.232-239, 2013.

[18] K. Kawamura, S. Nishikawa, K. Hirano, A. Ardianor, R. A. Nugroho, and S. Okada, "Large-scale screening of natural genetic resource in the hydrocarbon-producing microalga *Botrycoccus braunii* identified novel fast-growing strains," Scientific Report, vol. 11, no. 7368, 2021.

[19] H. Taherdoost, "Decision making using the analytic hierarchy process (AHP); a step by step decision approach," International Journal of Economics and Management System, vol. 2, Feb, pp.244–246, 2017.

[20] M. Brunneli, "Introduction to the analytic hierarchy process," SpringerBriefs in Operations Research, pp. 83. 978-3-319-12502-2 (electronic), 2015.

[21] R. W. Saaty, "The analytic hierarchy process-what it is and how it is used," Mathematical Modelling, vol. 9, no. 3–5, pp.161–176, 1987.

[22] Badan Pusat Statistik Kabupaten Cilacap, "Keadaan Suhu Udara/Air Temperature 2018-2020," Badan Pusat Statistik Kabupaten Cilacap, 2021. [Online]. Available: https://cilacapkab.bps.go.id/indicator/151/327/1/keadaan-suhu-udara-air-temperature.html. [Accessed: Oct. 3, 2021]

[23] V. Ashokkumar and R. Rengasamy, "Mass culture of *Botryococcus braunii Kutz*. under open raceway pond for biofuel production," Bioresource Technology, vol. 104, pp.394–399, 2012.

[24] S. S. Khichi, A. Anis, and S. Ghosh, "Mathematical modeling of light energy flux balance in flat panel photobioreactor for *Botryococcus braunii* growth, CO_2 biofixation and lipid production under varying light regimes," Biochemical Engineering Journal, vol. 134, pp.44–56, 2018.

[25] M. G. d. Reis, and A. Ribeiro, "Conversion factors and general equations applied in agricultural and forest meteorology," Agrometeoros, vol. 27, no. 2, pp.227–258, 2020.

[26] L. Marbelia, M. R. Bilad, I. Passaris, V. Discart, D. Vandamme, A. Beuckels, K. Muylaert, and I. F. J. Vankelecom, "Membrane photobioreactors for integrated microalgae cultivation and nutrient remediation of membrane bioreactors effluent," Bioresource Technology, vol. 163, pp.228–235, 2014.

[27] J. A. Ramirez, R. J. Brown, and T. J. Rainey, "A review of hydrothermal liquefaction bio-crude properties and prospects for upgrading to transportation fuels," Energies, vol. 8, no. 7, pp.6765–6794, 2015.

[28] N. Sharma, K. K. Jaiswal, V. Kumar, M. S. Vlaskin, M. Nanda, I. Rautela, M. S. Tomar, and W. Ahmad, "Effect of catalyst and temperature on the quality and productivity of HTL bio-oil from microalgae: A review," Renewable Energy, vol. 174, pp.810–822, 2021.

[29] R. Ren, X. Han, H. Zhang, H. Lin, J. Zhao, Y. Zheng, and H. Wang, "High yield bio-oil production by hydrothermal liquefaction of a hydrocarbon-rich microalgae and biocrude upgrading," Carbon Resources Conversion, vol. 1, no. 2, pp.153–159, 2018.

[30] M. Marsullo, A. Mian, A. V. Ensinas, G. Manente, A. Lazzaretto, and F. Marechal, "Dynamic modeling of the microalgae cultivation phase for energy production in open raceway ponds and flat panel photobioreactors," Frontiers in Energy Research, vol. 3, 41, 2015.

[31] R. Davis, A. Aden, and P. T. Pienkos, "Techno-economic analysis of autotrophic microalgae for fuel production," Applied Energy, vol. 88, no. 10, pp.3524–3531, 2011.

[32] J. W. Richardson, M. D. Johnson, X. Zhang, P. Zemke, W. Chen, and Q. Hu, "A financial assessment of two alternative cultivation systems and their contributions to algae biofuel economic viability," Algal Research, vol. 4, no. 1, pp.96–104, 2014.

[33] P. Lindblad, D. Fuente, F. Borbe, B. Cicchi, J. A. Conejero, N. Couto, H. Čelešnik, M.M. Diano, M. Dolinar, S. Esposito, C. Evans, E. A. Ferreira, J. Keller, N. Khanna, G. Kind, A. Landels, L. Lemus, J. Noirel, S. Ocklenburg, P. Oliveira, C. C. Pachecoc, J. L. Parker, J. Pereira, T. K. Pham, F. Pinto, S. Rexroth, M..Rögner, H. Schmitz, A. M. S. Benavides, M. Siuranan, P. Tamagnini, E. Touloupakis, G. Torzillo, J. F. Urchueguía, A. Wegelius, K. Wiegand, P. C. Wright, M. Wutschel, R. Wünschiers, "CyanoFactory, a European consortium to develop technologies needed to advance *Cyanobacteria* as chassis for production of chemicals and fuels," Algal Research, vol. 41, May, no. 101510, 2019.

[34] Y. Luo, P. Le-Clech, and R. K. Henderson, "Simultaneous microalgae cultivation and wastewater treatment in submerged membrane photobioreactors: A review," Algal Research, vol. 24, pp.425–437, 2017.

[35] K. Kumar, S.K. Mishra, A. Shrivastav, M. S. Park, and J. W. Yang, "Recent trends in the mass cultivation of algae in raceway ponds," Renewable and Sustainable Energy Reviews, vol. 51, pp.875–885, 2015.

[36] E. Sierra, F. G. Acien, J. M. Fernandez, J. L. Garcıa, C. Gonzalez, and E. Molina, "Characterization of a flat plate photobioreactor for the production of microalgae," Chemical Engineering Journal, vol. 138, pp.136–147, 2008.

[37] M. R. Bilad, D. Vandamme, I. Foubert, K. Muylaert, and I. F. J. Vankelecom, "Harvesting microalgal biomass using submerged microfiltration membranes," Bioresource Technology, vol. 111, pp.343–352, 2012.

[38] N. Norsker, M. J. Barbosa, M. H. Vermuë, and R. H. Wijffels, "Microalgal production — A close look at the economics," Biotechnology Advances, vol. 29, no.1, pp.24–27, 2011.

[39] A. K. S. Lau, M. R. Bilad, N. B. Osman, L. Marbelia, Z. A. Putra, N. A. H. M. Nordin, M. D. H. Wirzal, J. Jaafar, and A. L. Khan, "Sequencing batch membrane photobioreactor for simultaneous cultivation of aquaculture feed and polishing of real secondary effluent," Journal of Water Process Engineering, vol. 29, Mar., no. 100779, 2019.

[40] R. R. Narala, S. Garg, K. K. Sharma, S. R. Thomas-Hall, M. Deme, Y. Li and P. M. Schenk, "Comparison of microalgae cultivation in photobioreactor, open raceway pond, and a two-stage hybrid system," Frontiers in Energy Research, vol. 4, no. 29, 2016.

[41] M. Zhang, L. Yao, E. Maleki, B, Liao, H. Lin, "Membrane technologies for microalgal cultivation and dewatering: recent progress and challenges," Algal Research, vol. 44, no. 101686, 2019.

FREE 1 (2022) 31-37

Frontiers in Renewable Energy (FREE)

Journal homepage: www. https://jurnal.ugm.ac.id/v3/FREE/

Selection of Harvesting Technology for Botryococcus braunii as Feedstock of Bio-crude Oil Production

Abdul Rozaq Albaqi[1], Nugroho Dewayanto[1,2], Eko Agus Suyono[2,3], and Arief Budiman[2,4]

[1] Master Program in System Engineering, Universitas Gadjah Mada
Jalan Teknika Utara 3, Barek, Yogyakarta 55281, Indonesia
[2] Center of Excellence for Microalgae Biorefinery, Center for Energy Studies, Universitas Gadjah Mada
Sekip K1A, Kampus UGM, Yogyakarta 55281, Indonesia
[3] Faculty of Biology, Universitas Gadjah Mada
Jalan Teknika Selatan, Yogyakarta 55281, Indonesia
[4]Department of Chemical Engineering, Universitas Gadjah Mada
Jalan Grafika 2, Yogyakarta 55281

ARTICLE INFO

Article history:
Received 21 January 2022
Revised 4 February 2022
Accepted 8 April 2022
Available online 10 August 2022

Key words:
Microalgae harvesting, bio-crude oil, Analytic Hierarchy Process

ABSTRACT

The continuous increase in energy consumption of fossil fuels has led to the urgency of research and development in the field of renewable energy for the future. Meanwhile, microalgae such as Botryococcus braunii are among the renewable energy alternatives and a third-generation source of bio-crude oil, producing more biomass compared to others. However, the challenges that are usually encountered in the selection of an effective approach for microalgae harvesting are the small size of cells (3-30 µm) and the similarity between their densities and growth media. Therefore, this research aims to determine the appropriate microalgae harvesting technology for bio-crude oil production using the Analytical Hierarchy Process (AHP). Several potential harvesting technologies that have been used include centrifugation, filtration, inorganic and organic flocculation, bioflocculation, electrocoagulation, and flocculation-sedimentation. The results showed that the parameters considered include energy need (0.339), cost (0.214), risk of contamination (0.098), efficiency (0.133), technology availability (0.066), microalgae strain flexibility (0.079), and production time (0.071). Subsequently, the pairwise comparison of seven alternatives and criteria for each harvesting technology are compared. Based on the results, flocculation-sedimentation with a weight of 0.202 is the best alternative that can be recommended as a microalgae harvesting technology

I. INTRODUCTION

Microalgae are potential feedstocks for producing sustainable biofuels and other high-value products [1]. This is because their derivation does not interfere with food availability since they are obtained from non-food raw materials. Microalgae are a third-generation biofuel source with several advantages over terrestrial crops due to their high potential yield and relatively quicker

Peer review under responsibility of Frontiers in Renewable Energy (FREE).
*Corresponding author.
E-mail address: abudiman@ugm.ac.id (Arief Budiman)

growth rates [2]. Generally, microalgae are a group of micro plants that belong to the algae class, with diameters between 3-30 μm, and single cells as well as colonies living in freshwater and marine areas. Photosynthesis is carried out in microalgae to produce biomass, which absorbs nutrients and carbon dioxide quicker than other crops. They also play a role in 1/3 of the carbon fixation process that occurs in the world and produces approximately 70% of the oxygen in the atmosphere [2]. Meanwhile, the species used in this research was Botryococcus braunii, which is a green colony freshwater microalga that produces hydrocarbons [3] and is present in all climatic zones except Antarctica [4]. The content of carbon, hydrogen, and the high heating value (HHV) in the biomass of Botryococcus braunii at approximately 32.9–54.7 MJ/kg have a higher value than other types of microalgae [5]. Previous reports have shown that harvesting is a significant challenge that occurs in the use of microalgae as renewable energy. This is due to the small size of micro-algal cells (3-30 μm), low concentration of < 0.6 g/L, and the similarity of the density of the algal cells to the growth medium [6]. Harvesting is carried out by separating microalgae from their growth medium using a solid-liquid separation technique to process the biomass and produce useful products. This process uses several methods, namely chemical, mechanical, biological, electrical-based operations, and a combination of these procedures. Meanwhile, an ideal method must be suitable for most of the microalgae types, achieve high biomass recovery, and use minimal energy with nominal operative cost [7]. Therefore, reducing the harvesting costs is important for the sustainable and inexpensive production of bio-crude oil.

Microalgae harvesting methods have advantages and disadvantages, which are distinguished by their efficiency, time and energy needs, investment, operational, and chemical costs. To achieve economically viable and sustainable production, the cost of these steps needs to be reduced [10]. Therefore, this research aims to select the most pre ferred harvesting technology for bio-crude oil production. The development of a systematic multi-criteria decision-making (MCDM) was carried out using Analytic Hierarchy Process (AHP) to evaluate the technology alternatives in microalgae harvesting. One of the strengths of AHP is combining both quantitative and qualitative information to identify the preferred alternative. The qualitative data are quantified through a survey from algal experts. In its development, AHP is used to determine the priority of choices with many criteria and as an alternative method to solve various problems [9].

II. METHODOLOGY

AHP has been widely applied and extensively investigated in several fields since its initial introduction by Thomas L. Saaty in 1980. In this research, the AHP method was used to determine the harvesting technology, which has a set of criteria to select the alternatives that were determined previously. It allows for bias in making decisions by combining logical considerations and values. Furthermore, its basic principle includes breaking the problem into separate elements, setting the priority of each component or aspect, and weighing the priority set logically and consistently [8]. The first step in the AHP method was to compile a hierarchy of research schemes at several levels. Level 1 was the purpose of this research, namely the appropriate microalgae harvesting technology. Level 2 was the 7 criteria used, which include energy need, cost, risk of contamination, efficiency, technology availability, microalgae strain flexibility, and production time, while level 3 was the alternatives to be selected. The alternative used consisted of centrifugation, cross-flow filtration, organic and inorganic flocculation, bioflocculation electrocoagulation, and flocculation-sedimentation. The objectives, criteria, and alternatives are shown in Figure 1.

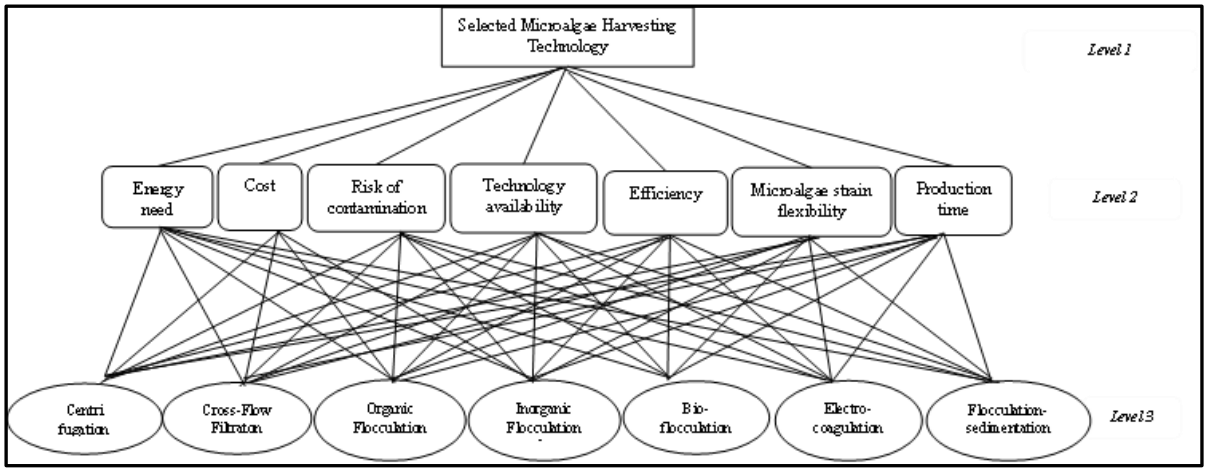

Figure 1. Analytic hierarchy process structure

The second step was to carry out pairwise comparisons between criteria and alternatives, which were scaled from 1 to 9 [9], as shown in Table 1. This was followed by the calculation of eigenvectors or the weight value of the criteria and consistency tests. The final stage was to calculate the weight value and arrange the priority sequence of each alternative.

Table 1. Hierarchy Rating Scale [6]

Interest	Variable definitions	Explanation
1	Just as important	The two elements have the same effect.
3	A little bit more important	Slightly siding with one of the elements
5	More important	Strongly siding with one element.
7	Very important	One element is very influential and its dominance is evident.
9	Absolutes are more important	One of the more essential elements of the partner is very clear.
2,4,6,8	The middle value of the assessment above	The value is given when there is doubt between the two options.
Reciprocal	When the ratio between the elements i and j yields one of the values above, the ratio between the elements j to i will produce the opposite value.	

III RESULTS AND DISCUSSION

An example of AHP is shown with the best microalgae harvesting technology (Figure 1). Based on previous research [10] – [13], there are several potential microalgae harvesting technologies, namely centrifugation, cross-flow filtration, organic and inorganic flocculation, bioflocculation, electrocoagulation, and flocculation-sedimentation

3.1 Criteria Weight Calculation (Level 2)

In this research, a pairwise comparison was carried out to indicate the preference for each criterion. The seven criteria compared were energy need, cost, risk of contamination, efficiency, technology availability, microalgae strain flexibility, and production time. The exact method was carried out by calculating the average of respondent data, followed by the consistency calculation as shown in Table 2.

Table 2. Pairwise comparison matrix for criteria

Criteria	Energy need	Cost	Risk of contamination	Efficiency	Technology availability	Microalgae strain flexibility	Production time
Energy need	1	3	3	5	4	3	3
Cost	1/3	1	4	4	2	3	2
Risk of contamination	1/3	1/4	1	3	1	1	1
Efficiency	1/5	1/4	1/3	1	1	1	1
Technology availability	1/4	1/2	1	1	1	4	3
Microalgae strain flexibility	1/3	1/3	1	1	1/4	1	2
Production time	1/3	1/2	1	1	1/3	1/2	1

The eigenvectors or the weight value of the criteria was calculated followed by consistency tests as shown in Table 3. Based on the calculations, the parameters that can be used as a basis for consideration in making decisions are energy need (0.339), followed by cost (0.214), efficiency (0.133), risk of contamination (0.098), microalgae strain flexibility (0.079), production time (0.071), and technology availability (0.066) as the last priority.

Table 3. Weight of criteria

Criteria	Energy need	Cost	Risk of contamination	Efficiency	Technology availability	Microalgae strain flexibility	Production time
Weight	0.339	0.214	0.098	0.066	0.133	0.079	0.071
Inconsistency				0.076			

3.2 Calculation of Alternative Local Weights Against Criteria (Level 3)

The calculation of the weight alternative against the criteria is also carried out to determine the best option for solving the problem. The value of the criteria for energy consumption, cost, efficiency, and production time is obtained from previous research [10]-[17], as shown in Table 4. Meanwhile, the criteria for risk of contamination, technology availability, and microalgae strain flexibility were obtained based on expert judgment. The qualitative decisions are scaled in pairs as shown in Table 1 by assessing the importance of an element compared to other components. The pairwise comparison from the assessment result of the three qualitative criteria is shown in Tables 5 to 7. The weighting result for this level is shown in Table 8.

Table 4. Determined matrix for microalgae harvesting techniques

Criteria	Energy need (kWh/ m^3)	Cost (USD)	Efficiency (%)	Production time (min)
Centrifugation	5.50	500	90.0	10
Crossflow-filtration	2.06	200	92.5	10
Inorganic flocculation	4.00	300	95.0	40
Organic Flocculation	4.00	300	99.0	30
Bioflocculation	2.00	250	95.0	20
Electrocoagulation	3.00	400	90.0	20
Flocculation-sedimentation	2.50	250	99.0	25

Table 5. Pairwise comparison matrix for risk of contamination criteria

Risk of contamination	Centrifugation	Crossflow-filtration	Inorganic flocculation	Organic Flocculation	Bio flocculation	Electro-coagulation	Flocculation-sedimentation
Centrifugation	1	1/3	1	1/3	2	2	1/4
Crossflow-filtration	3	1	2	1/2	1/2	3	1/3
Inorganic flocculation	1	1/2	1	1/3	1	3	1/3
Organic Flocculation	3	2	3	1	2	4	1
Bioflocculation	1/2	2	1	1/2	1	2	1
Electro-coagulation	1/2	1/3	1/3	1/4	1/2	1	1/3
Flocculation-sedimentation	4	3	3	1	1	3	1

Table 6. Pairwise comparison matrix for technology availability criteria

Technology availability	Centrifugation	Crossflow-filtration	Inorganic flocculation	Organic Flocculation	Bio flocculation	Electro-coagulation	Flocculation-sedimentation
Centrifugation	1	3	2	2	3	3	1
Crossflow-filtration	1/3	1	1	1	1	2	1/3
Inorganic flocculation	1/2	1	1	3	3	3	1
Organic Flocculation	1/2	1	1/3	1	3	3	2
Bioflocculation	1/3	1	1/3	1/3	1	1	1/3
Electro-coagulation	1/3	1/2	1/3	1/3	1	1	1/3
Flocculation-sedimentation	1	3	1	1/2	3	3	1

Table 7. Pairwise comparison matrix for microalgae strain flexibility criteria

Microalgae strain flexibility	Centrifugation	Crossflow-filtration	Inorganic flocculation	Organic Flocculation	Bio flocculation	Electro-coagulation	Flocculation-sedimentation
Centrifugation	1	3	1/2	2	3	3	1/2
Crossflow-filtration	1/3	1	1/3	1/3	1	2	1/3
Inorganic flocculation	2	3	1	2	3	3	2
Organic Flocculation	1/2	3	1/2	1	3	3	2
Bioflocculation	1/3	1	1/3	1/3	1	2	1/3
Electro-coagulation	1/3	1/2	1/3	1/3	1/2	1	1/3

Microalgae strain flexibility	Centrifugation	Crossflow-filtration	Inorganic flocculation	Organic Flocculation	Bio flocculation	Electro-coagulation	Flocculation-sedimentation
Flocculation-sedimentation	2	3	1/2	1/2	3	3	1

Table 8. Calculation of weights between alternatives to criteria

Criteria	Energy need	Cost	Risk of contamination	Efficiency	Technology availability	Microalgae strain flexibility	Production time
Centrifugation	0.061	0.079	0.099	0.241	0.032	0.182	0.257
Crossflow-filtration	0.207	0.217	0.138	0.104	0.032	0.070	0.166
Inorganic flocculation	0.108	0.136	0.094	0.192	0.155	0.261	0.074
Organic Flocculation	0.108	0.136	0.239	0.158	0.297	0.182	0.105
Bioflocculation	0.189	0.167	0.134	0.065	0.155	0.070	0.133
Electro-coagulation	0.121	0.113	0.051	0.058	0.032	0.053	0.133
Flocculation-sedimentation	0.207	0.151	0.246	0.183	0.297	0.182	0.133
CR	0.007	0.015	0.073	0.061	0.001	0.049	0.014

As shown in Table 8, the calculation of the weights alternatives against criteria was carried out according to AHP. For every alternative, the value from Table 8 was multiplied by the individual criterion weight as indicated in Table 3. The sum of these products was the scores for each alternative and the highest score was selected as the best.

The Centrifugation score is calculated as follows:

(0.339 x 0.061) + (0.214 x 0.079) + (0.098 x 0.099) + (0.066 x 0.241) + (0.133 x 0.032) + (0.079 x 0.182) + (0.071 x 0.257) = 0.100

The score for other alternatives is shown in Table 9. The results showed that flocculation-sedimentation is the most preferred harvesting technology followed by organic flocculation, crossflow filtration, bioflocculation, inorganic flocculation, centrifugation, and electrocoagulation.

Table 9. Weighting and ranking of harvesting alternatives

Alternative	Weight	Ranking
Flocculation-sedimentation	0.202	1
Organic Flocculation	0.161	2
Crossflow-filtration	0.158	3
Bioflocculation	0.153	4
Inorganic flocculation	0.134	5
Centrifugation	0.100	6
Electro-coagulation	0.092	7

IV. CONCLUSION

A multi-criteria decision-making model using the AHP approach was developed to evaluate seven harvesting technology, namely centrifugation, filtration, inorganic and organic flocculation, bioflocculation, electrocoagulation, and flocculation-sedimentation. Based on the data analysis, it was discovered that the level of influence of the criteria to be considered include energy needs (0.339), cost (0.214), risk of contamination (0.098), efficiency (0.133), technology availability (0.066), microalgae strain flexibility (0.079), and production time (0.071). The result showed that flocculation-sedimentation is the most preferred harvesting technology with a weight of 0.202, followed by organic flocculation, crossflow filtration, bioflocculation, inorganic flocculation, centrifugation,

and electrocoagulation with 0.161, 0.100, 0.158, 0.153, 0.134, 0.100, and 0.092, respectively.

References

[1] Guldhe A., Singh B., Rawat I., Ramluckan K., Bux F.,"Efficacy of drying and cell disruption techniques on lipid recovery from microalgae for biodiesel production", Fuel, 128, 46-52, 2014.

[2] Viswanath B, Mutanda T, White S, Bux F., "The microalgae – a future source of biodiesel". Dynam Biochem, Process Biotechnol Mol Biol, 4(1):37–47, 2010.

[3] A. R. Rao, G. A. Ravishankar, and R. Sarada, "Cultivation of green alga Botryococcus braunii in raceway , circular ponds under outdoor conditions and its growth, hydrocarbon production," Bioresource Technology, vol. 123, pp.528–533, 2012.

[4] M. B. Tasic, L. F. R. Pinto, B. C. Klein, V. B. Veljković, and R. M. Filho, "Botryococcus braunii for biodiesel production," Renewable and Sustainable Energy Reviews, vol. 64, pp.260–270, 2016.

[5] J. Jin, C. Dupré, K. Yoneda, M. M. Watanabe, J. Legrand, and D. Grizeau, "Characteristics of extracellular hydrocarbon-rich microalga Botryococcus braunii for biofuels production: Recent advances and opportunities," Process Biochemistry, vol. 51, no. 11, pp.1866–1875, 2016.

[6] Christenson L, and Sims R., "Production and harvesting of microalgae for wastewater treatment, biofuels, and bioproducts", Biotechnol Adv, 29:686–702, 2011.

[7] Mathimani T, and Mallick N., "A comprehensive review on harvesting of microalgae for biodiesel – key challenges and future directions", Renew Sustain Energy Rev; 91:1103–20, 2018.

[8] T. L. Saaty, 1986, "Decision Making for Leaders, The Analytical Hierarchy Process for Decision in Complex World", Pitsburgh: University of Pitsburgh, 1986.

[9] T. L. Saaty, "Decision making with the analytic hierarchy process,"Int. J. Services Science 1, no. 1, 85-98, 2008.

[10] Unay, E., Ozkaya, B., and Yoruklu, H. C., "A multicriteria decision analysis for the evaluation of microalgal growth and harvesting", Chemosphere, 279, 130561, 2021.

[11] Ortiz, A., García-Galán, M. J., García, J., and Díez-Montero, R., "Optimization and operation of a demonstrative full scale microalgae harvesting unit based on coagulation, flocculation and sedimentation", Separation and Purification Technology, 259 (November 2020), 2021.

[12] Tan, J., Low, K. Y., Sulaiman, N. M. N., Tan, R. R., & Promentilla, M. A. B., "Fuzzy analytical hierarchy process (AHP) for multi-criteria selection in drying and harvesting process of microalgae system", Chemical Engineering Transactions, 45, 829–834, 2015.

[13] Al-hattab, M., Ghaly, A., Hammouda, A., "Microalgae harvesting methods for industrial production of biodiesel: critical review and comparative analysis", J. Fund. Renew. Energy Appl. 5, 154, 2015.

[14] Fasaei, F., Bitter, J. H., Slegers, P. M., and van Boxtel, A. J. B., "Techno-economic evaluation of microalgae harvesting and dewatering systems", Algal Research, 31, 347–362, 2018.

[15] Ferreira, J., de Assis, L. R., Oliveira, A. P. de S., Castro, J. de S., and Calijuri, M. L., "Innovative microalgae biomass harvesting methods: Technical feasibility and life cycle analysis", Science of the Total Environment, 746, 2020.

[16] Li, S., Hu, T., Xu, Y., Wang, J., Chu, R., Yin, Z., Mo, F., and Zhu, L., "A review on flocculation as an efficient method to harvest energy microalgae: Mechanisms, performances, influencing factors and perspectives", Renewable and Sustainable Energy Reviews, 131(May), 2020.

[17] Nwokoagbara, E., Olaleye, A. K., and Wang, M., "Biodiesel from microalgae: The use of multi-criteria decision analysis for strain selection", Fuel, 159, 241–249, 2015.

FREE 1 (2022) 38-43

Frontiers in Renewable Energy (FREE)

Journal homepage: www. https://jurnal.ugm.ac.id/v3/FREE/

Designing PEM Electrolysis-Based Hydrogen Reactors in The Area of Baron Beach of Yogyakarta, Indonesia

Danu Nugroho[1], Arief Budiman[2*], Eko Agus Suyono[2,3], and Wahyu Wilopo[3*]

[1] Master Program in System Engineering, Universitas Gadjah Mada
Jalan Teknika Utara 3, Barek, Yogyakarta 55281, Indonesia
[2] Department of Geological Engineering, Faculty of Engineering, Universitas Gadjah Mada
Jalan Grafika 2, Yogyakarta 55281
[3]Department of Chemical Engineering, Universitas Gadjah Mada
Jalan Grafika 2, Yogyakarta 55281

ARTICLE INFO

Article history:
Received 18 Febryary 2022
Revised 24 March 2022
Accepted 24 June 2022
Available online 10 August 2022

Key words:
PEM Electrolyzer,
Thermodynamic, Hydrogen,
Electrolysis, Optimum.

ABSTRACT

This study aimed to design a PEM electrolysis-based hydrogen reactor and the potential for hydrogen production at Baron Beach, Gunung Kidul, Yogyakarta. Based on the calculation done at the initial process, the electrical energy potentially generated from renewable energy, such as wind, waves, and solar, reached 10.7 MW. This study also investigated the effect of reactor operating temperature on reactor efficiency and hydrogen production. A numerical thermodynamic approach was applied in the design process. The model, validated by laboratory experiments by other institutions, was in good agreement with previous research with an error value of 13%. The temperature range was dynamically limited from 30 to 80°C. The optimum operating conditions occurred when the temperature was set at 80 °C with a reactor efficiency, a water consumption rate, and a hydrogen production capacity of 76.3%, 2.817 kg/hour, and 250.42 kg/hour, respectively. The raw material, namely seawater, was processed using the reverse osmosis method. Ten reactors (with 13 cells per reactor) were installed in parallel.

I. INTRODUCTION

Baron Beach in Yogyakarta, Indonesia, has a unique contour with a basin surrounded by rocks. It is suitable for constructing power plants. The potential for electrical energy from wave, wind, and solar power in the vicinity of the area reaches 10.7 MW. This value, if produced in the absence of local demand and export, can be a potential commodity to be converted into hydrogen as an environmentally friendly fuel through water electrolysis that has been widely applied as fuel cells in the industrial and automotive fields [1][2]. Hydrogen itself is a substance that has many strategic functions in the chemical industry, like being a raw material for ammonia, methanol, oil refining, and various other chemicals [3].

Many researchers have designed renewable energy-based water electrolysis reactors with various approach methods, including modeling with an empirical and computational approach using Aspen and MATLAB software. [4] modeled a combination of an 18 kW wind turbine and 12 kW solar cell-Alkaline Water Electrolyzer with the help of MATLAB software.

Peer review under responsibility of Frontiers in Renewable Energy (FREE).
*Corresponding author.
E-mail address: abudiman@ugm.ac.id (Arief Budiman)

The parameters studied were the effect of hydrogen reactor temperature and on hydrogen production. They concluded that the higher the temperature, the efficiency of hydrogen production increased, which was accompanied by an increase in current density and a decrease in electric voltage. [5] modeled a PEM Electrolyzer with Aspen Custom Modeler software. In such modeling, they did not consider reactor geometry but did the effect of operating conditions, namely temperature and pressure, on hydrogen production. They found that an increase in operating pressure will only increase the voltage, while an increase in temperature will increase the current density only.

In 2018 and 2020, Sánchez [7] modeled a 15 kW-Alkaline Water Electrolyzer with the help of MATLAB software and the Aspen Custom Modeler. In his two studies, he developed a semi-empirical model compiled with MATLAB to be a computational model with the Aspen Custom Modeler. His modeling included a hydrogen reactor and its supporting process units. He found that as the operating temperature rose from 50 to 80°C, the voltage dropped, as did the stack power required for electrolysis. Meanwhile, the hydrogen production rate decreased when the temperature increased because the Faraday efficiency decreased and more hydrogen molecules crossed to the oxygen side. At a pressure of 5-9 bars, the stack stress did not increase significantly and did not affect the rate of hydrogen production. However, the higher the operating pressure, the lower the purity of the hydrogen. The purpose of this study is effect of operating temperature on the PEM Electrolyzer performance was studied using an empirical approach.

II. METHODOLOGY

Water electrolysis means separating water molecules into hydrogen and oxygen through an electrochemical reaction with the addition of electrical energy [6]. An electric current flow between two separate electrodes immersed in the electrolyte to increase the ionic conductivity. The reactions that occur at the electrodes are formulated in Eq (1) - (3) [8]. However, these reaction are occured in base environment.

$$\text{Anode} : 2OH^- \rightarrow H_2O + 1/2O_2 + 2e^- \quad (1)$$

$$\text{Cathode: } 2H_2O + 2e^- \rightarrow H_2 + 2OH^- \quad (2)$$

$$\text{Overall} : H_2O \rightarrow H_2 + 1/2O_2 \quad (3)$$

There are several types of water electrolysis technologies, including Alkaline Water Electrolyzer (AEL), Proton Exchange Membrane (PEM) Electrolyzer, and Solid Oxide Electrolyzer (SOEL) [9]. PEM is the most attractive technology to be applied in the industrial sector because it has a compact design, high current density, higher stability, higher gas purity, and high hydrogen production rate and is the most suitable to be developed commercially. Therefore, in this study, the PEM Electrolysis-based hydrogen reactor was chosen.

Thermodynamically, the minimum energy required to break a water molecule can be calculated from the Gibbs free energy as a function of the reversible voltage. The reversible voltage itself is the minimum voltage of the cell for allowing the electrolysis process to occur at standard temperature and pressure.

$$V_{rev} = \frac{\Delta G^\circ}{nF} = 1.23V \quad (4)$$

where:

ΔG° = standard Gibbs free energy (J/mol)

n = the number of electrons involved

F = Faraday constant (96500 C/mol)

V_{rev} = reversible voltage (V)

However, when the water molecules separate, a certain amount of entropy is released, so the total energy required for the electrolysis process is the enthalpy change of the process. So Equation (4) changes to:

$$\Delta G^\circ = \Delta H^\circ - Q = \Delta H^\circ - T.\Delta S^\circ$$

$$V_{rev} = \frac{\Delta H^\circ}{nF} = \frac{\Delta G^\circ}{nF} + \frac{T\Delta S^\circ}{nF} = 1.48V \quad (5)$$

where:

ΔH° = enthalpy change (J/mol)

ΔS° = entropy change (J/mol.K)

T = operating temperature (K)

In fact, the reversible voltage is not only affected by temperature and pressure but also by the catalytic properties of the electrode, the diffusivity of the membrane, and the internal resistance of the cell. So the cell voltage follows the following equation:

$$V_{cell} = V_{rev}(T) + \eta_{electrode} + \eta_\Omega \quad (6)$$

where:

Vcell = Cell voltage (V)

ηelectrode = Kinetic resistance

η_Ω = Ohmic loses

According to Carmo [10], the typical operating temperature of a PEM electrolyzer ranges from 20 to 80°C. In this study, variations in operating temperature on the performance of the PEM electrolyzer reactor were studied using a thermodynamic approach to determine the optimum operating conditions. The thermodynamic approach was carried out empirically with the following assumptions:

- The effect of pressure was ignored
  According to Marangio *et al*. [11], pressurized PEM electrolyzers have several weaknesses, including: the phenomenon of cross-permeate or water that is not converted because it crosses directly through the membrane to the cathode side, corrosion, brittleness of reactor material by hydrogen, and cell instability.
- Uniform temperature in every cell.
- The heat lost to the surroundings was ignored.
- The mass transfer resistance or gas diffusivity to the membrane was ignored.
- The catalytic or kinetic properties of the electrode were ignored.
- Ohmic losses were constant
  In this study, the type of membrane used was Nafion 117 with the value of ohmic losses considered constant and not a function of temperature. According to Slade *et al*. [12], Nafion 117 membrane has an ohmic resistance value of 0.15 V

So Equation (6) can be simplified to Equation (7)

$$V_{cell} = V_{rev}(T) + 0.15 \quad (7)$$

where V_{rev} is a function of temperature at constant pressure by following the following equation.

$$V_{rev} = 1.5184 - 1.5421.10^{-3}T + 9.523.10^{-5}T\,lnT + 9.84.10^{-8}T^2 \quad (8)$$

By combining Equations (7) and (8), the equation to calculate the cell voltage for the electrolysis process is as follows:

$$V_{cell} = 1.6684 - 1.5421.10^{-3}T + 9.523.10^{-5}T\,lnT + 9.84.10^{-8}T^2 \quad (9)$$

The hydrogen production capacity of an electrolyzer is closely related to cell current and Faraday efficiency. Faraday efficiency is the relationship between the actual and theoretical hydrogen production rates caused by standby current losses or parasitic currents. According to research by Barbir [13] and Gorgun [14], Faraday's efficiency value for PEM electrolyzer is more than 99%. Hydrogen production capacity and electrolyzer feed water requirements can be calculated by the following equation:

$$fH_2 = \frac{n_{cell}\,I_{cell}}{2F}\eta_F \quad (10)$$

$$fH_2O = 1.25\frac{n_{cell}\,I_{cell}}{2F}\eta_F \quad (11)$$

where:

f_{H2} = hydrogen production rate

f_{H2O} = feed water consumption rate

n_{cell} = number of cells

I_{cell} = cell current

η_F = Faraday efficiency

F = Faraday constant (96485 C/mol)

where the cell current can be calculated by the following equation, where P is the power generation (Watts):

$$I_{cell} = \frac{P}{V_{cell}} \quad (12)$$

After calculating with a thermodynamic approach, the results of these calculations were validated with experimental results. Validation was done by comparing the calculated Vcell value and experimental results at various temperatures. Validation accuracy was calculated based on error following the following equation:

$$Error = \frac{experiment - calculation}{experiment}\ x\ 100\% \quad (13)$$

The experimental results were taken from the PEM Electrolyzer facility for Hydrogen production at UPCT (Technical University of Cartagena) with the following specifications [15].

- Capasity = 1 kW
- Number of cells = 12
- Membrane = Nafion, 50cm2
- Number of reactor = 1 unit

III RESULTS AND DISCUSSION

As shown in equation (9), the cell voltage (Vcell) is the reverse voltage required to start an electrolysis process. The Vcell itself is the voltage required to counter resistance such as thermodynamic resistance (operating conditions), kinetic resistance (catalytic properties of the material), and mass transfer resistance (membrane diffusivity), and ohmic losses. In this study, the kinetic resistance-mass transfer was neglected and the ohmic losses were considered constant so that Vcell was considered as a function of temperature only. The results of calculating the Vcell and Icell values at various operating temperatures is presented in Figures 1 and 2.

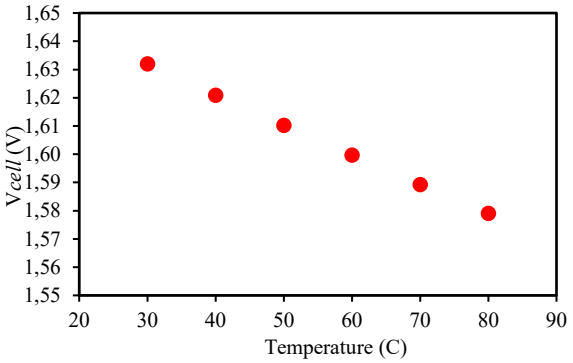

Figure 1. Effect of Temperature on Cell Voltage

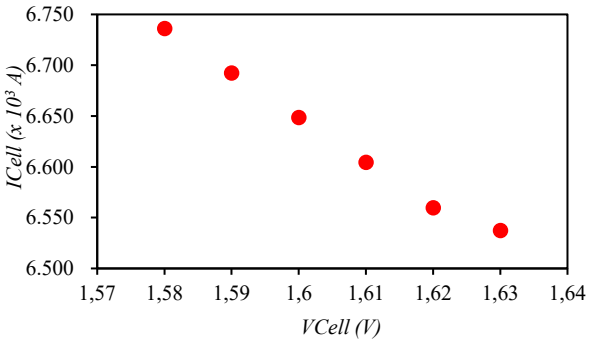

Figure 2. Effect of Cell Voltage on Cell Current

Figure 1 and 2 show that the increase in temperature decreases Vcell and increases Icell so that the rate of hydrogen production also increases according to Equation 10 as presented in Figure 3.

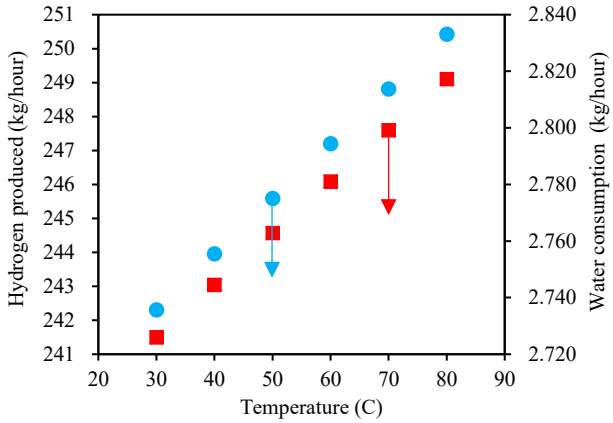

Figure 3. Hydrogen Production Rate and Water Consumption Rate at various operating temperatures

These data were following the report of the research conducted by Colbertaldo et al. [5], Sánchez et al. [7], and Sánchez et al. [16]. However, there was a difference between the results of the thermodynamic approach and those of the experiments, as presented in Figure 4. At the same temperature, the experimental Vcell was higher than the calculation one using the thermodynamic approach due to the presence of obstacles such as kinetic resistance and mass transfer, which were taken into account in the experiment. Thus, to carry out the electrolysis process, a higher Vcell value was needed. Figure 4 also shows that the higher the temperature rise, the smaller the difference in the Vcell values based on the experimental results and the approach results.

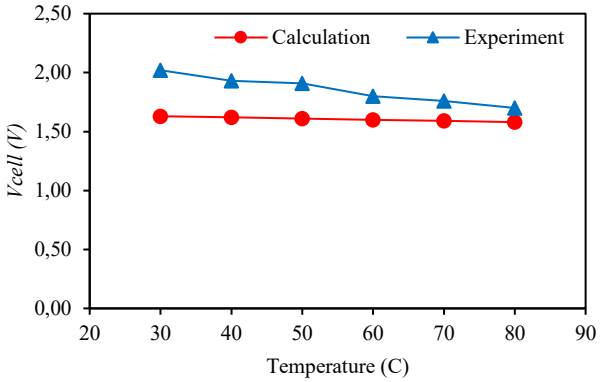

Figure 4. Comparison of Vcells based on Experiment vs Calculation

Figure 5 presents a process flow diagram for the hydrogen reactor design in this study. From this figure, the reactor heat and mass balance can be arranged so that the reactor efficiency can be calculated by the following equation:

$$\eta = \frac{n_{H_2}\, HHV_{H_2}}{P + Q_{cell} + Q_{H_2O}}\ x\ 100\% \qquad (14)$$

where
n_{H2} = Mol of hydrogen produced
HHV_{H2} = High heating value of hidrogen (286 kJ/mol)
P = Power required (kW)
Q_{cell} = Heat required for electrolysis (48.6kJ/mol H_2O) [12]
Q_{H2O} = The heat required to raise water temperature

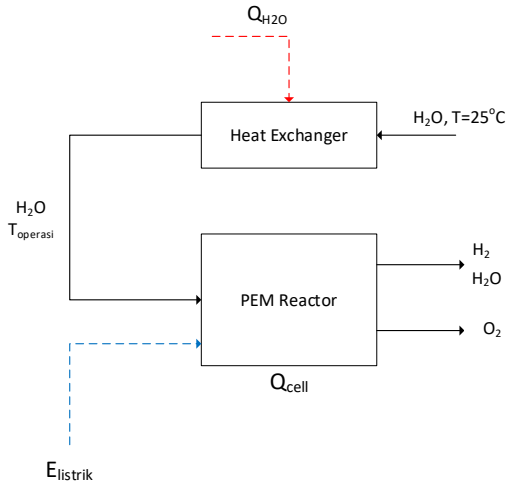

Figure 5. Reactor Design Process Flowchart

Through Equation (14), the calculation of the efficiency of the electrolysis process at various temperatures is presented in Figure 6. The highest efficiency was obtained at an operating temperature of 80°C. Thermodynamically, at this temperature, the electrolysis process should be carried out.

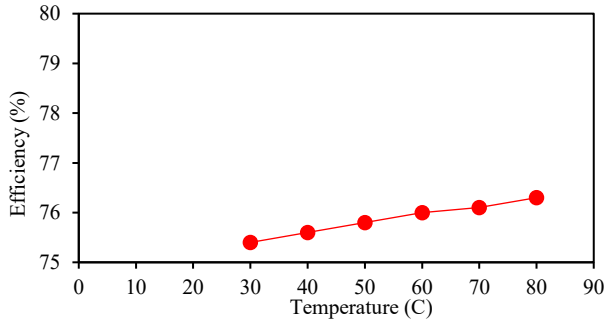

Figure 6. Reactor efficiency at various temperatures

Based on the calculation of the thermodynamic approach, the hydrogen reactor designed in this study was as follows:

Reactor type	= Proton Exchange
Membrane Toperating	= 80°C
Number of reactors	= 10 units
Configuration	= parallel
Number of cells	= 13
Membrane type	= Nafion 117
Active Area	= 50 cm^2
Current Density	= 1.2 A/cm^2

IV. CONCLUSION

From this research's results, it can be concluded that,

a. The PEM Electrolysis-based hydrogen reactors designed with the empirical thermodynamic approach were quite appropriate, as evidenced by an error value of 13%.
b. The optimum production could be obtained at an operating temperature of 80oC with a hydrogen production capacity, system efficiency, and an electric power input of 250.42 kg/hour, 76.3%, and 10.7 MW, respectively.
c. The designed hydrogen reactors consisted of 10 units installed in parallel. The number of cells in each reactor was 13.

References

[1] Yeh, S., D. H. Loughlin, C. Shay and C. Gage., "An Integrated Assessment of the Impacts of Hydrogen Economy on Transportation, Energy Use, and Air Emissions", *Proceedings of the IEEE,* 94 pp 1838-1851, 2006.

[2] Veziroglu, A. and R. Macario., "Fuel cell vehicles: State of the art with economic and environmental concerns", *International Journal of Hydrogen Energy,* 36 pp 25-43, 2011.

[3] Arregi, A., M. Amutio, G. Lopez, J. Bilbao and M. Olazar, "Evaluation of thermochemical routes for hydrogen production from biomass: A review", *Energy Conversion and Management*, 165 pp 696-719, 2018.

[4] Huang, P.-H., J.-K. Kuo and Z.-D. Wu., "Applying small wind turbines and a photovoltaic system to facilitate electrolysis hydrogen production", *International Journal of Hydrogen Energy,* 41 pp 8514-8524, 2016.

[5] Colbertaldo, P., S. L. G. Alaez and S. Campanari., "Zero-dimensional dynamic modeling of PEM electrolyzers", *Energy Procedia,* 142 pp 1468-1473, 2017.

[6] Burton, N. A., R. V. Padilla, A. Rose and H. Habibullah., "Increasing the efficiency of hydrogen production from solar powered water electrolysis", *Renewable and Sustainable Energy Reviews*, 135, 2021.

[7] Sánchez, M., E. Amores, L. Rodríguez and C. Clemente-Jul., "Semi-empirical model and experimental validation for the performance evaluation of a 15kW alkaline water electrolyzer", *International Journal of Hydrogen Energy,* 43 pp 20332-20345, 2018.

[8] Shiva Kumar, S. and V. Himabindu, "Hydrogen production by PEM water electrolysis – A review", *Materials Science for Energy Technologies,* 2 pp 442-454, 2019.

[9] Buttler, A. and H. Spliethoff., "Current status of water electrolysis for energy storage, grid balancing and sector coupling via power-to-gas and power-to-liquids: A review", *Renewable and Sustainable Energy Reviews,* 82 pp 2440-2454, 2018.

[10] Carmo, M., D. L. Fritz, J. Mergel and D. Stolten., "A comprehensive review on PEM water electrolysis", *International Journal of Hydrogen Energy,* 38 pp 4901-4934, 2013.

[11] Marangio, F., M. Santarelli and M. Cali, "Theoretical model and experimental analysis of a high pressure PEM water electrolyser for hydrogen production", *International Journal of Hydrogen Energy,* 34 pp 1143-1158., 2009.

[12] Slade, S., Campbell, S. A., Ralph, T. R. & Walsh, F. C., "Ionic Conductivity of an Extruded Nafion 1100 EW Series of Membranes", *Journal of The Electrochemical Society*, 149 pp A1556-A1564, 2002.

[13] Barbir, F., "PEM electrolysis for production of hydrogen from renewable energy sources", *Solar Energy,* 78 pp 661-669, 2005.

[14] Gorgun, H., "Dynamic modelling of a proton exchange membrane (PEM) electrolyzer", *International Journal of Hydrogen Energy,* 31 pp 29-38, 2006.

[15] Maeda, T., Ito. H, Akai. M, Hasegawa. Y, Hasegawa. R and Hada. Y., "Control method and basic characteristics of photovoltaic PEM electrolyzer system", *Proc Renewable Energy Chiba*, pp 22, 2006.

[16] Sánchez, M., E. Amores, D. Abad, L. Rodríguez and C. Clemente-Ju., "Aspen Plus model of an alkaline electrolysis system for hydrogen production", *International Journal of Hydrogen Energy,* 45 pp 3916-3929, 2020.

Center for Energy Studies
Universitas Gadjah Mada
Sekip Blok K1.A, Jalan Bhinneka Tunggal Ika
Yogyakarta, Indonesia, 55281

ISSN 2961-7855